

# Self-Gravitating Magnetic Monopoles and Dyons in String-Inspired Models: Structure and Stability

Nick E. Mavromatos,<sup>1,2,\*</sup> Sarben Sarkar,<sup>2,†</sup> and Dionysios P. Theodosopoulos<sup>3,‡</sup>

<sup>1</sup>*Physics Division, School of Applied Mathematical and Physical Sciences,  
National Technical University of Athens, 15780 Zografou Campus, Athens, Greece.*

<sup>2</sup>*Theoretical Particle Physics and Cosmology Group, Department of Physics,  
King's College London, London WC2R 2LS, United Kingdom.*

<sup>3</sup>*Texas Center for Cosmology and Astroparticle Physics,  
Weinberg Institute for Theoretical Physics, Department of Physics,  
The University of Texas at Austin, Austin, TX 78712, USA*

We present classical solutions for magnetic monopoles and dyons induced by global monopoles for string-inspired models, in the presence of gravity. Two distinct scenarios are analyzed. In the first, magnetic monopoles arise from the coupling of a non-trivial massless dilaton field to the electromagnetic (EM) sector. In the second, dyonic solutions emerge in the presence of a non-trivial Kalb-Ramond (KR) axion field *and* a massless dilaton field, which couples the KR and EM sectors. In both models, the monopole and dyon configurations originate from a global monopole associated with the spontaneous breaking of a global  $O(3)$  symmetry. The EM sector is described by Born-Infeld electrodynamics, ensuring regularity of the fields at the core of the monopole and a finite self-energy. The resulting solutions represent particle-like configurations with a well-defined core and positive ADM (Arnowitt-Deser-Misner) mass, and are shown to satisfy all standard energy conditions. Interestingly, we also demonstrate the existence of a minimum nonzero magnetic charge in the limiting case of a magnetic monopole with vanishing mass, in which the monopole is held up entirely by its magnetic charge and the de Sitter core pressure. We also discuss stability criteria for our magnetic-monopole and dyon solutions. In particular, we first demonstrate that the mechanical-stability criteria for these solutions are satisfied. Namely, these require the finiteness of the total force components (as defined by means of the stress-energy tensor) and also the outward-pointing nature of the radial component, which indicates the avoidance of collapse. Next we analyse the dynamical (linear perturbative) stability of the self-gravitating Born-Infeld monopole and dyon solutions within Einstein-Born-Infeld-dilaton-axion theory. Working in the exterior analytic region of the monopole, we introduce gauge-invariant electromagnetic-perturbation variables following the Gervalle-Volkov framework. These are projected onto helicity eigenstates  $\psi_{\pm}$  using a null tetrad (adapted to a spherically symmetric background). The linearised equations reduce to a Schrödinger-like radial system governed by a self-adjoint Sturm-Liouville operator. We demonstrate that both monopole and dyonic configurations are linearly stable against electromagnetic perturbations in the exterior region, with dyons exhibiting a birefringent helicity structure due to axion-induced mixing.

## I. INTRODUCTION

Although magnetic monopoles (MM) are theoretical solutions of the Euler-Lagrange equations of some microscopic field-theory models, there is still no experimental evidence [1] for their existence, despite intensive searches, in both the Cosmos and at colliders. There may be various reasons for this. One could be that such configurations arise in Grand Unified Theory (GUT) models [2, 3], in which the electromagnetic  $U(1)$  gauge group is part of a larger group, *e.g.* a GUT gauge group, or is embedded in an  $SU(2)$  gauge group in Georgi-Glashow-type field theories [4]. In the GUT case, the MM solutions have masses close to the inflationary scale (that is, close to grand unification scale (GUT),  $M \gtrsim 10^{14}$  GeV). Such MM have been diluted by inflation, and, thus, their observation is practically impossible. Another reason for the non-observation of such MM, even if they had relatively low masses (of the order of the electroweak scale), is their compositeness. Such (solitonic) MM solutions consist of gauge-bosons and (charged) Higgs quanta; their production in current or future colliders is exponentially suppressed [5], despite their theoretical justification as being solutions of field equations in specific models [6–8] (based on the Standard-Model (SM) gauge group, or appropriate extensions [9]). In collider kinematics, a composite monopole, such as a *'t Hooft–Polyakov* or *Cho–Maison* monopole, is not created as an elementary point particle. Rather, it would have to be assembled from many Higgs and gauge-field quanta into a coherent classical soliton. This produces an entropy-mismatch penalty:

\* nikolaos.mavromatos@kcl.ac.uk

† sarben.sarkar@kcl.ac.uk

‡ d.theodosopoulos@utexas.edu

among all possible high-multiplicity final states with the same energy, only an exponentially small fraction have the ordered field configuration of a monopole. The corresponding rate is therefore expected to be suppressed by a factor of order

$$\exp\left(-\frac{4}{\alpha}\right) \sim 10^{-240},$$

where  $\alpha \simeq 1/137$  is the fine-structure constant. Collider production of such composite monopoles is consequently unobservable, even when their masses are kinematically accessible.

The situation is radically different in the early Universe. The entropy-suppression argument applies to collider production because a few incoming quanta must organise themselves into a coherent, extended soliton. During a cosmological symmetry-breaking phase transition, however, the relevant Higgs field is already a macroscopic classical field distributed throughout space. Monopoles are then formed by the ordering of the vacuum itself, rather than by the rare assembly of many particles into a special final state. Suppose a symmetry group  $G$  is spontaneously broken to a subgroup  $H$ . The degenerate vacuum states form the vacuum manifold

$$\mathcal{M}_{\text{vac}} = \frac{G}{H}. \quad (1.1)$$

At temperatures above the critical temperature  $T_c$ , the symmetry is restored and the Higgs expectation value vanishes. As the Universe cools through  $T_c$ , the Higgs field rolls away from the symmetric point and chooses a vacuum value on  $\mathcal{M}_{\text{vac}}$ . The crucial point is causality. At the time of the transition, two regions separated by more than a horizon distance cannot communicate. Therefore they cannot coordinate their choices of Higgs orientation. The Higgs field chooses its vacuum direction independently in different causal domains. If the correlation length is denoted by  $\xi$ , then one expects roughly independent vacuum choices over regions of size  $\xi$ , with

$$\xi \lesssim H^{-1}(T_c), \quad (1.2)$$

where  $H(T_c)$  is the Hubble rate at the transition. For monopoles the relevant topology is

$$\pi_2(\mathcal{M}_{\text{vac}}) \neq 0. \quad (1.3)$$

In the simplest case,

$$\pi_2(\mathcal{M}_{\text{vac}}) = \mathbb{Z}. \quad (1.4)$$

This means that maps from a two-sphere in physical space into the vacuum manifold can carry an integer winding number. Around a would-be monopole core, the Higgs field defines a map

$$S_{\text{space}}^2 \longrightarrow \mathcal{M}_{\text{vac}}. \quad (1.5)$$

If this map has non-zero winding number, the Higgs field cannot be smoothly deformed everywhere into a single vacuum orientation. At the centre of the configuration the Higgs field must leave the vacuum manifold, typically passing through  $\phi = 0$ . That point is the monopole core.

This is the Kibble mechanism [10]. Random choices of vacuum orientation in neighbouring domains make it unavoidable that some closed surfaces in space enclose non-trivial winding. The monopole is therefore not produced by a rare collision process; it is a topological remnant of the phase transition. A crude estimate of the initial monopole density follows immediately. If approximately one independent field orientation is chosen per correlation volume  $\xi^3$ , then the initial number density is of order

$$n_M(t_c) \sim \xi^{-3}. \quad (1.6)$$

Since causality gives  $\xi \lesssim H^{-1}(T_c)$ , one often writes the rough Kibble estimate as

$$n_M(t_c) \sim H^3(T_c), \quad (1.7)$$

up to numerical factors and model-dependent corrections. Subsequent monopole–antimonopole annihilation, entropy production, inflationary dilution, or plasma effects can reduce this abundance, but the important point is that the initial formation probability is not Boltzmann suppressed. Thus the early-Universe phase transition avoids the collider entropy-mismatch penalty. A composite monopole does not have to be assembled from many uncorrelated quanta. Instead, it forms as a classical field defect because the Higgs vacuum orientation cannot be chosen consistently across all causally disconnected domains.

Hence the unsuppressed channels for producing composite magnetic monopoles are (i) symmetry-breaking phase transitions in the early Universe and (ii) the dual Schwinger mechanism in ultra-strong magnetic fields, both of which circumvent the exponential suppression factor characteristic of collider environments [11–14], which catalyze the unsuppressed production of MM. This suppression does not apply to elementary (structureless) Dirac-type MM [15, 16], behaving as sources of singular magnetic fields (magnetic poles), although their mass needs to be made finite by mechanism which go beyond the standard model [17]. We characterise these as ordinary monopoles [18] since:

- They are *point-like*: the monopole magnetic field is exactly that of an isolated electric charge but with roles of  $\mathbf{E}$  and  $\mathbf{B}$  swapped,

$$\mathbf{B}(\mathbf{r}) = \frac{g}{4\pi} \frac{\mathbf{r}}{r^3}, \quad g = n g_{\text{D}}, \quad n \in \mathbb{Z}.$$

- Dirac’s quantisation condition,  $e g = \frac{n}{2} \hbar c$ , fixes the fundamental charge  $g_{\text{D}}$  and ensures single-valued electron wavefunctions.
- It carries *no internal structure*: there is no Higgs field or non-Abelian gauge profile inside a finite radius.

The monopoles that we will construct will approximate such monopoles at late epochs (once the relevant dilaton time gradients fade after the formation epoch, right after the symmetry breaking phase transition)<sup>1</sup>.

Since gravity can affect their masses, because of gravitational binding energy, MM solutions need, for completeness, to incorporate gravity. The masses compared to the Minkowski spacetime cases, could be reduced. This is necessary for experimental verification, and also essential when considering MM in the early Universe. Self-gravitating magnetic monopoles in string-inspired effective theories provide a natural setting in which nontrivial topology, nonlinear gauge dynamics, and spacetime backreaction are realised within a single framework. The inclusion of dilaton and Born–Infeld sectors, motivated by low-energy string theory [19], can lead to finite-energy monopole solutions with regular cores and nontrivial asymptotic structure [20]. The Born–Infeld (BI) form of nonlinear electrodynamics is singled out both by its string-theoretic origin and by its regularisation of the divergent electromagnetic self-energy of a monopole. This allows solutions with a finite, positive ADM mass (the total gravitational energy seen at infinity). Moreover, as discussed in [20], Born-Infeld regularised theories can also admit structureless Dirac-type MM solutions, which can be produced at colliders without suppression, as mentioned above.

It is our purpose to discuss such solutions, which stem from non-gauged global monopoles, but are promoted to MM through appropriate mediator fields, for example scalar dilatons or pseudoscalar axions, that characterise microscopic string models [21]. One such case [22] arose in string-inspired models in which a MM arises from global monopoles [23], as a result of the coupling of a (constant, but non-trivial) dilaton scalar field to both the electromagnetic Maxwell part of the effective action and the kinetic terms of the Kalb-Ramond (KR) field strength of the spin-one massless antisymmetric tensor of the massless bosonic string gravitational multiplet [24, 25]. In (3+1) spacetime dimensions, after string compactification, the KR field is dual to a massless pseudoscalar (KR axion) field, and thus the induced MM has an axion charge, that is quantized in order for the Dirac charge quantization condition [16] to be satisfied. The gravitational stability and finiteness of total energy for such MM have been discussed [26], while their sizes and masses have been estimated, in terms of the parameters of the model.

In this work we treat other interesting cases in effective string-inspired actions containing gravity, where global monopoles with dilaton or axion (KR) charges are promoted to MM via appropriate interactions. Two families of such solutions are constructed (partly numerically) within an action containing gravity, a global- $O(3)$  Higgs triplet, a dilaton  $\Phi$ , an axion (KR pseudoscalar)  $b$ , and Born–Infeld electrodynamics [19]. The first family consists of purely magnetic monopoles stabilised by a *non-constant* dilaton with charge  $\zeta$ ;<sup>2</sup> the second extends these to dyons when the axion field has a  $bF\tilde{F}$  coupling (where  $F$  denotes the electromagnetic field strength and  $\tilde{F}$  its dual). Both families are shown to possess positive ADM mass and a regular de Sitter core, with the form of the metric, dilaton, and Higgs profiles verified partly numerically.

A central question for such configurations is their stability, both mechanical in the sense discussed in [27], and dynamical. While the existence of regular solutions is by now established, their mechanical stability viewed as solitonic objects (similar to configurations appearing in nuclear matter [28]) needs to be examined first. If the total internal force is finite and its radial component is directed inwards, towards the centre of the monopole, then this would imply the tendency of the system to collapse leading to mechanical instability. By contrast a finite total force, radially pointing outwards, would indicate mechanical stability. Moreover, stability under linear perturbations of such

<sup>1</sup> Although the self-gravitating Born–Infeld monopole has a finite-radius core and scalar hair, its *external* electromagnetic field is identical to that of a pointlike Dirac monopole.

<sup>2</sup> The dilaton charge is the coefficient of the  $1/r$  *fall-off* of the dilaton field at large radial distance.

solutions needs also to be studied, and provides important complementary information.<sup>3</sup> This task is complicated in our case, owing to nonlinear constitutive relations and the coupling between the gauge, scalar, and gravitational sectors.

In contrast with simple single-field stability problems, the Born–Infeld–dilaton–axion monopole does not generally lead to a single elementary effective potential  $V(r)$ . In the simplest case one would obtain a Schrödinger-type equation of the form<sup>4</sup>

$$-\frac{d^2 u}{dr_*^2} + V(r)u = \omega^2 u, \quad (1.8)$$

where  $V(r)$  is a known scalar function. If  $V(r)$  is manifestly non-negative, stability can often be inferred directly. In the present problem the situation is more complicated. The static, spherically symmetric metric is written as

$$ds^2 = -B(r)dt^2 + \frac{dr^2}{A(r)} + R^2(r)d\Omega^2. \quad (1.9)$$

and the background contains several non-trivial radial functions,

$$A(r), \quad B(r), \quad R(r), \quad \Phi(r), \quad b(r), \quad F_{\mu\nu}(r), \quad (1.10)$$

The remaining radial functions are matter fields. The dilaton profile

$$\Phi = \Phi(r) \quad (1.11)$$

changes the effective electromagnetic coupling, since the Born–Infeld sector contains factors such as

$$e^{\Phi}, \quad e^{-2\Phi}. \quad (1.12)$$

Therefore the electromagnetic perturbations propagate in a medium whose effective coupling varies with radius. In the dyonic case there is also a Kalb–Ramond axion profile

$$b = b(r), \quad (1.13)$$

which couples through the pseudoscalar term

$$b F_{\mu\nu} \tilde{F}^{\mu\nu}. \quad (1.14)$$

Because  $b(r)$  is radius-dependent, it induces radius-dependent mixing between electric and magnetic perturbations, or equivalently between the two helicity sectors. Finally,

$$F_{\mu\nu} = F_{\mu\nu}(r) \quad (1.15)$$

denotes the background electromagnetic field strength. In the purely magnetic case its non-zero component is

$$F_{\theta\phi} = Q_m \sin \theta, \quad (1.16)$$

whereas in the dyonic case there is also an electric component,

$$F_{tr}(r) = e^{\Phi(r)} \frac{Q_e - (b(r) - b_0)Q_m}{R^2(r)}. \quad (1.17)$$

Consequently, the perturbation equations have coefficients depending on

$$A(r), \quad B(r), \quad R(r), \quad \Phi(r), \quad b(r), \quad F_{\mu\nu}(r). \quad (1.18)$$

They are therefore not governed by a simple potential such as

$$V(r) = \frac{\ell(\ell+1)}{r^2}. \quad (1.19)$$

<sup>3</sup> Such linear-stability analyses is a standard tool in the case of solitonic field-theoretic solutions in curved spacetimes, *e.g.* black holes with Higgs hair in spontaneously broken SU(2) gauge theories [29]. Needless to say, though, that linear stability by itself does not provide a proof of absolute stability, and must be extended to the case beyond linear perturbations, which algebraically is often a very complicated task, or combined with other methods to get complementary information (*e.g.* Catastrophe theory, as in the case of [29]).

<sup>4</sup> Here  $r_*$  is the tortoise co-ordinate used in black hole physics.

The electromagnetic perturbations also probe the Born–Infeld constitutive tensor. The latter depends nonlinearly on the background field invariants

$$F_{\mu\nu}F^{\mu\nu}, \quad F_{\mu\nu}\tilde{F}^{\mu\nu}. \quad (1.20)$$

Consequently, after harmonic decomposition, the perturbation equations do not reduce to a single closed-form potential. Instead, they take the schematic Sturm–Liouville form

$$\mathcal{L}\Psi = -\frac{d}{dr_*}\left(P(r)\frac{d\Psi}{dr_*}\right) + \mathbf{V}(r)\Psi, \quad (1.21)$$

where  $\Psi$  denotes the vector of radial gauge-invariant perturbation amplitudes and  $\mathbf{V}$  is a matrix. The tortoise coordinate  $r_*$  is defined by

$$\frac{dr_*}{dr} = \frac{1}{\sqrt{A(r)B(r)}}. \quad (1.22)$$

Equivalently,

$$r_*(r) = \int^r \frac{d\bar{r}}{\sqrt{A(\bar{r})B(\bar{r})}}. \quad (1.23)$$

In particular, the perturbation equations do not, in general, reduce to a simple closed-form potential, and must instead be analysed through their structural properties. Specifically, we consider *dynamical stability* of electromagnetic perturbations of a self-gravitating monopole background and show that the problem reduces to a self-adjoint Sturm–Liouville system of the above type. For the purely magnetic monopole, the helicity sectors decouple identically, and the analysis reduces to a scalar radial equation defined on a piecewise background consisting of an *interior* de Sitter core and an exterior monopole geometry. For gravitating solitons this analysis is non-trivial because gauge redundancy, constraint equations, and mode mixing of different helicities in curved backgrounds all conspire to obscure the physical degrees of freedom if one were to work with the perturbation of the vector potential.

Although the effective radial potential in the Sturm–Liouville equation cannot be written in closed analytic form, its qualitative structure is sufficient to control the spectrum. In particular, the interior region is governed by a positive centrifugal barrier, while the exterior potential exhibits a repulsive divergence near the inner boundary and a non-negative asymptotic tail. We formulate the stability problem in variational terms and show that, under mild and physically well-motivated assumptions on subleading contributions from the Born–Infeld and dilaton sectors, no negative modes arise. The systematic framework for addressing this question is due to Gervalle–Volkov (GV) [30], and was developed originally for perturbations of electroweak monopoles (Cho–Maison (CM)) [6]. Recently, this method has been applied [17] also to study the stability of the BI regularised CM [20, 31]. We note that stringent lower bounds on the mass of such BI monopoles can be imposed at current and future colliders [32–34]. The overlap with the GV framework is methodological rather than physical: as in GV and in the BI-regularised electroweak monopole analysis of [17], we use complex-tetrads, spin-weighted harmonics, gauge-fixing, and constraint-elimination machinery to reduce the perturbation problem to a self-adjoint radial Sturm–Liouville system. The novelty here is its application to a self-gravitating dilaton-axion Born–Infeld monopole/dyon background, where the constitutive tensor induces a helicity-based radial system and, in the dyonic case, a nontrivial mixing term  $W(r)$ . The GV approach works directly with gauge-invariant variables built from the field-strength perturbation  $\delta F_{\mu\nu}$ , projects these onto helicity eigenstates using a null tetrad, and exploits the constitutive tensor  $\chi^{\mu\nu}{}_{\rho\sigma}$  of nonlinear electrodynamics to reduce the linearised stability equations to a Schrödinger-like radial system of Sturm–Liouville type. For static backgrounds the resulting operator is self-adjoint, immediately implying a real spectrum and hence stability.

The present paper provides a self-contained implementation of the GV analysis for our solutions. Our aim is threefold: (i) to derive the gauge-invariant helicity variables from first principles in an accessible manner; (ii) to reduce the linearised equations explicitly to the Sturm–Liouville form and determine the effective potentials; (iii) to use the structure of the resulting operator to establish linear stability for both monopoles and dyons. For completeness, we also check that the energy conditions of such solutions are satisfied.

The paper is organised as follows. Section II gives a brief review of the self-gravitating global monopole of [23]. Section III discusses magnetic monopoles induced by global monopoles with a dilaton charge, and Section IV treats the dyonic generalisation with dilaton and axion charges in models incorporating Born–Infeld electrodynamics. Section V contains the full stability analysis. We first establish mechanical stability and the energy conditions (Section V A). Section V B then develops the formalism for piecewise linear dynamical stability, introducing gauge-invariant perturbation variables, the helicity projections  $\psi_{\pm}$ , and the self-adjoint Sturm–Liouville structure of the perturbation

equations. Section VC applies this framework to the explicit solutions: Section VC1 treats the purely magnetic monopole (where the helicity sectors decouple and the effective potential is positive definite) and Section VC2 treats the dyonic case, deriving the helicity-mixing term and establishing stability from self-adjointness and an explicit bound on the off-diagonal potential. Finally, Section VI summarises our conclusions. Appendix A gives the detailed derivation of the radial potentials for the monopole case, and Appendix B provides supplementary material on mechanical stability.

## II. GLOBAL MONOPOLES

Global monopoles (GMs) are topological defects arising from the spontaneous breaking of a global O(3) symmetry. The gravitational field of a GM in Einstein gravity was first derived in Ref. [23], considering a Higgs triplet  $\chi^a$  (with  $a = 1, 2, 3$ ) and a Higgs potential that breaks the global O(3) symmetry:

$$S = \int d^4x \sqrt{-g} \left[ \frac{R}{16\pi G} + \mathcal{L}_{GM} \right], \quad (2.1)$$

$$\mathcal{L}_{GM} = -\frac{1}{2}(\nabla_\mu \chi^a)(\nabla^\mu \chi^a) - \frac{\lambda}{4}(\chi^a \chi^a - \eta^2)^2, \quad (2.2)$$

where  $g = \det(g_{\mu\nu})$ , and  $R$  is the Ricci scalar<sup>5</sup>. In the region where the O(3) symmetry is spontaneously broken, the spacetime metric reads

$$ds^2 = -\left(1 - 8\pi G\eta^2 - \frac{2GM}{r}\right) dt^2 + \frac{dr^2}{1 - 8\pi G\eta^2 - \frac{2GM}{r}} + r^2(d\theta^2 + \sin^2\theta d\phi^2), \quad (2.3)$$

where  $\eta$  determines a deficit solid angle. Specifically, after appropriate coordinate redefinitions, the spacetime (2.3) exhibits a conical singularity associated with the angular deficit factor  $1 - 8\pi G\eta^2$  [22, 23].

A physically acceptable GM spacetime should be free of horizons and curvature singularities. In that sense, the authors of Ref. [35] proposed that the monopole possesses a de Sitter (dS) core of radius  $\delta$ , within which the metric is given by

$$ds^2 = -\left(1 - \frac{2\pi G\lambda\eta^4}{3}r^2\right) dt^2 + \frac{dr^2}{1 - \frac{2\pi G\lambda\eta^4}{3}r^2} + r^2(d\theta^2 + \sin^2\theta d\phi^2). \quad (2.4)$$

Imposing the Israel conditions [36], which require continuity of the metric and its first derivative across the core boundary, yields the ADM mass and core radius

$$M = -\frac{16\pi}{3} \frac{\eta}{\sqrt{\lambda}}, \quad \delta = \frac{2}{\eta\sqrt{\lambda}}. \quad (2.5)$$

The negative ADM mass implies repulsive gravitational effects, rendering the GM configuration unstable. This result was further confirmed numerically in Ref. [35], where the mass was found to be

$$M = -6\pi \frac{\eta}{\sqrt{\lambda}}, \quad (2.6)$$

indicating that the instability persists beyond the analytic approximation. This motivates the search for extended frameworks in which the monopole mass can become positive, as we explore in the following sections.

## III. MAGNETIC MONOPOLES FROM GLOBAL MONOPOLES WITH A DILATON CHARGE

In this section we construct a magnetically charged monopole solution generated by a GM coupled to gravity, in the presence of a dilaton field and Born–Infeld non-linear electrodynamics. Our motivation is twofold. First, previous

---

<sup>5</sup> Our conventions and definitions throughout this work are:  $(-, +, +, +)$  for the signature of the metric, the Riemann tensor is defined as  $R^\lambda{}_{\mu\nu\sigma} = \partial_\nu \Gamma^\lambda{}_{\mu\sigma} - \Gamma^\rho{}_{\mu\sigma} \Gamma^\lambda{}_{\rho\nu} - (\nu \leftrightarrow \sigma)$ , and the Ricci tensor and scalar are given by  $R_{\nu\alpha} = R^\lambda{}_{\nu\lambda\alpha}$  and  $R = g^{\mu\nu} R_{\mu\nu}$  respectively. Also we work in natural units  $\hbar = c = 1$ . Newton's constant  $G$  is retained explicitly.

studies have shown that suitable extensions of the gravitational sector can convert the negative-mass behaviour of ordinary GMs into physically acceptable configurations with positive ADM mass. Second, in string-inspired settings the dilaton naturally couples to the electromagnetic (EM) sector, while the Born–Infeld action provides a non-linear completion of Maxwell theory that regularises the monopole self-energy. Against this background, we investigate whether a GM can source a magnetic charge through its coupling to the dilaton and thereby give rise to a regular, self-gravitating magnetic monopole with positive ADM mass. We first formulate the Einstein-frame field equations, then derive approximate analytic solutions inside and outside the monopole core, and finally compare them with numerical results.

A GM solution with positive ADM mass in an extended Gauss–Bonnet theory of gravity was derived in [37]. Moreover, a magnetically charged GM solution with positive ADM mass was obtained in a string-inspired gravitational theory [22, 26], where the magnetic charge originates from a Kalb–Ramond axion-like field and ensures the positivity of the ADM mass. Motivated by this result, we seek a magnetic monopole solution sourced by a GM minimally coupled to gravity, in which the magnetic charge is associated with a dilaton charge and leads to a positive ADM mass. The EM sector of the Lagrangian will be described by the string inspired Born-Infeld (BI) electrodynamics.

One of the distinctive features of string/brane-induced non-linear electrodynamics is that higher-order corrections in the Maxwell tensor can be resummed into a closed-form expression, namely the BI Lagrangian [38–43]. This arises from the resummation of open-string excitations, for example those attached to D3-brane worlds in the D-brane formulation of string theory. In this case, the three-dimensional brane world-volume leads to the Dirac–Born–Infeld (DBI) action (see [44–46] and references therein). In such constructions, BI electrodynamics in four spacetime dimensions originates from the higher-dimensional ( $d = 10$ ) superstring action, either through compactification or by restriction to the world-volume of a D3-brane. Importantly, in all string-inspired scenarios the BI Lagrangian couples to the inverse of the open-string coupling,  $g_s = e^\phi$ , where  $\phi$  denotes the dimensionless dilaton field. Consequently, the effective four-dimensional action in a curved background metric (in the Jordan or  $\sigma$ -model frame)  $g_{\mu\nu}^J$  takes the form

$$S_{\text{BI}}^J = -T_4^2 \int d^4x e^{-\phi} \sqrt{\text{Det}(-g_{\mu\nu}^J + T_4^{-1} \mathcal{F}_{\mu\nu})}, \quad (3.1)$$

where  $\mathcal{F}_{\mu\nu}$  is the Maxwell tensor  $\mathcal{F}_{\mu\nu} = \partial_\mu A_\nu - \partial_\nu A_\mu$ , and  $\mathcal{T}_4 = \frac{1}{2\pi\alpha'} = \frac{M^2}{2\pi}$  is the (open) string tension, with  $\alpha' = M_s^{-2}$  the Regge slope and  $M_s$  the string mass scale, which in general is different from the four-dimensional Planck scale.

Under the assumption of a constant dilaton and flat Minkowski spacetime, the Born–Infeld (BI) parameter  $\mathcal{T}_4^2$  can be constrained in collider experiments through light-by-light scattering, a process that is now experimentally established at the LHC (see [47–49]). In particular, such scattering studies [32] provide a lower bound  $\mathcal{T}_4 \gtrsim 100$  GeV. Within string theory, this translates into a (weak) lower limit on the string mass scale,  $M_s \gtrsim 0.25$  TeV. Current LHC searches in extra-dimensional scenarios further strengthen this bound to  $M_s \gtrsim \mathcal{O}(10)$  TeV, with forecasts for future colliders such as the FCC predicting significantly higher limits [33]. Embedding the BI framework into curved spacetime, while fully accounting for dilaton effects, opens an entirely new avenue for testing non-linear electrodynamics through the full machinery of modern gravitational experiments.

Beyond the brane DBI action (3.1), one may also consider higher-order derivative corrections in effective low-energy field theories arising from closed strings, such as the heterotic string [50]. Unlike the DBI brane or open-string case, these corrections do not resum into a closed-form expression for the gauge sector. Nevertheless, extensions of the BI effective action have been proposed in curved (3 + 1)-dimensional spacetimes, incorporating dilaton couplings to the electromagnetic fields in a BI-type non-linear electrodynamics (NED) framework [51–53]. Passing into the Einstein frame in four dimensions, via the transformation of the metric:  $g_{\mu\nu}^J \rightarrow g_{\mu\nu} = e^{-2\phi} g_{\mu\nu}^J$ , we write for the gravitational action (in units  $c = 1$ )

$$S = \int d^4x \sqrt{-g} \left[ \frac{R}{16\pi G} - \frac{1}{32\pi G} \nabla^\mu \Phi \nabla_\mu \Phi + \frac{1}{16\pi} \mathcal{L}_{\text{BI}} \right], \quad (3.2)$$

$$\mathcal{L}_{\text{BI}} = 4\beta_{\text{BI}} e^{\gamma\Phi} \left( 1 - \sqrt{1 + \frac{e^{-2\gamma\Phi}}{2\beta_{\text{BI}}} \mathcal{F}^2 - \frac{e^{-4\gamma\Phi}}{16\beta_{\text{BI}}^2} (\mathcal{F}\tilde{\mathcal{F}})^2} \right), \quad (3.3)$$

where we have redefined the dilaton field  $\phi \rightarrow \Phi/2$ ,  $\tilde{\mathcal{F}}_{\mu\nu} = \frac{1}{2} \epsilon_{\mu\nu\rho\sigma} \mathcal{F}^{\rho\sigma}$  is the dual of the Maxwell tensor, with  $\epsilon_{\mu\nu\rho\sigma}$  the fully antisymmetric Levi-Civita tensor,  $\gamma$  denotes the dilaton coupling, and  $\beta_{\text{BI}}$  is the generalized BI parameter, with mass dimension +2. In the string case,  $\beta_{\text{BI}}$  is identified with  $\mathcal{T}_4^2$ . To ensure consistency with the  $\mathcal{O}(\alpha')$  Maxwell terms of the heterotic string effective action [50], namely  $e^{-\Phi} \mathcal{F}^2$ , we will fix  $\gamma = 1$ .

We seek magnetically charged GM solutions in the following string-inspired gravitational theory:

$$S = \int d^4x \sqrt{-g} \left[ \frac{R}{16\pi G} + \mathcal{L}_{\text{GM}} - \frac{1}{32\pi G} \nabla^\mu \Phi \nabla_\mu \Phi + \frac{1}{16\pi} \mathcal{L}_{\text{BI}} \right], \quad (3.4)$$

where  $\mathcal{L}_{\text{GM}}$  is the standard GM Lagrangian given in Eq. (2.2). The equations of motion read

$$\square \chi^a = \lambda \chi^a (\chi^a \chi^a - \eta^2), \quad (3.5)$$

$$\nabla_\mu \left[ e^\Phi \frac{-e^{-2\Phi} \mathcal{F}^{\mu\nu} + \frac{1}{4\beta_{\text{BI}}^2} e^{-4\Phi} (\mathcal{F}_{\rho\sigma} \tilde{\mathcal{F}}^{\rho\sigma}) \tilde{\mathcal{F}}^{\mu\nu}}{\sqrt{1 + \frac{e^{-2\Phi}}{2\beta_{\text{BI}}} \mathcal{F}^2 - \frac{e^{-4\Phi}}{16\beta_{\text{BI}}^2} (\mathcal{F}\tilde{\mathcal{F}})^2}} \right] = 0, \quad (3.6)$$

$$\square \Phi = -4G e^\Phi \beta_{\text{BI}} \left( 1 - \sqrt{1 + \frac{e^{-2\Phi}}{2\beta_{\text{BI}}} \mathcal{F}^2 - \frac{e^{-4\Phi}}{16\beta_{\text{BI}}^2} (\mathcal{F}\tilde{\mathcal{F}})^2} \right) - 4G e^\Phi \beta_{\text{BI}} \frac{\frac{e^{-2\Phi}}{2\beta_{\text{BI}}} \mathcal{F}^2 - \frac{2e^{-4\Phi}}{16\beta_{\text{BI}}^2} (\mathcal{F}\tilde{\mathcal{F}})^2}{\sqrt{1 + \frac{e^{-2\Phi}}{2\beta_{\text{BI}}} \mathcal{F}^2 - \frac{e^{-4\Phi}}{16\beta_{\text{BI}}^2} (\mathcal{F}\tilde{\mathcal{F}})^2}}, \quad (3.7)$$

$$\mathcal{E}_{\mu\nu} : R_{\mu\nu} - \frac{1}{2} g_{\mu\nu} R = 8\pi G T_{\mu\nu}, \quad (3.8)$$

where

$$T_{\mu\nu} = T_{\mu\nu}^{\text{Higgs}} + T_{\mu\nu}^{\text{EM}} + T_{\mu\nu}^\Phi, \quad (3.9)$$

with

$$T_{\mu\nu}^{\text{Higgs}} = g_{\mu\nu} \left( -\frac{1}{2} (\nabla_\mu \chi^a) (\nabla^\mu \chi^a) - \frac{\lambda}{4} (\chi^a \chi^a - \eta^2)^2 \right) + \partial_\mu \chi^a \partial_\nu \chi^a, \quad (3.10)$$

$$T_{\mu\nu}^{\text{EM}} = g_{\mu\nu} \frac{e^\Phi}{4\pi} \beta_{\text{BI}} \left( 1 - \sqrt{1 + \frac{e^{-2\Phi}}{2\beta_{\text{BI}}} \mathcal{F}^2 - \frac{e^{-4\Phi}}{16\beta_{\text{BI}}^2} (\mathcal{F}\tilde{\mathcal{F}})^2} \right) + \frac{e^\Phi}{4\pi} \frac{e^{-2\Phi} \mathcal{F}_\mu{}^\rho \mathcal{F}_{\nu\rho} - \frac{e^{-4\Phi}}{2\beta_{\text{BI}}} (\mathcal{F}\tilde{\mathcal{F}}) \mathcal{F}_\nu{}^\rho \tilde{\mathcal{F}}_{\mu\rho}}{\sqrt{1 + \frac{e^{-2\Phi}}{2\beta_{\text{BI}}} \mathcal{F}^2 - \frac{e^{-4\Phi}}{16\beta_{\text{BI}}^2} (\mathcal{F}\tilde{\mathcal{F}})^2}}, \quad (3.11)$$

$$T_{\mu\nu}^\Phi = -\frac{g_{\mu\nu}}{32\pi G} (\partial\Phi)^2 + \frac{1}{16\pi G} \partial_\mu \Phi \partial_\nu \Phi. \quad (3.12)$$

Seeking for a static and spherically symmetric solution with a magnetic charge, we assume that  $\Phi = \Phi(r)$ , and introduce the ansätze

$$ds^2 = -B(r) dt^2 + \frac{dr^2}{A(r)} + R^2(r) (d\theta^2 + \sin^2 \theta d\phi^2), \quad (3.13)$$

$$\mathcal{F}_{\theta\phi} = -\mathcal{F}_{\phi\theta} = R^2(r) W(r) \sin \theta, \quad (3.14)$$

where all the other components of the EM strength are zero.

The global  $O(3)$  symmetry in Eq. (3.4) is spontaneously broken due to the Higgs potential. In the broken symmetry phase the Higgs triplet satisfies the equation

$$\chi^a \chi^a = \eta^2. \quad (3.15)$$

This condition defines a two-dimensional submanifold of the three-dimensional field space of  $\chi^a$ , which is homeomorphic to  $S^2$ . The three components  $\chi^a$  lie on a sphere of radius  $\eta$ , and therefore the vacuum manifold  $M_{\text{vac}} \simeq S^2$  has a non-trivial second homotopy group,  $\pi_2(M_{\text{vac}}) = \mathbb{Z}$ . Consequently, the vacuum manifold allows for the formation of topologically stable monopole defects. Seeking spherically symmetric solutions, we adopt the following ansatz for the Higgs triplet

$$\chi^a = \eta h(r) \frac{x^a}{r}, \quad x^a x^a = r^2, \quad (3.16)$$

such that  $h(r) \rightarrow 1$  as  $r \rightarrow \infty$  and  $h(r) \rightarrow 0$  as  $r \rightarrow 0$ .

The EM equations of motion are identically satisfied. The remaining equations can be solved by specifying the function  $W(r)$  in the form

$$W(r) = \frac{Q_m}{R^2(r)} , \quad (3.17)$$

which corresponds to the standard magnetic monopole configuration in BI electrodynamics. To solve the equations of motion, we assume a monopole structure similar to that introduced in Ref. [35], in which the monopole has a core of radius  $\delta$ . Outside the monopole core ( $r > \delta$ ), the global  $O(3)$  symmetry is spontaneously broken, and hence  $h(r) = 1$ . Moreover, far from the core the magnetic field is weak, and Born–Infeld electrodynamics reduces to Maxwell electrodynamics. Therefore, the dilaton equation and the stress-energy tensor of the electromagnetic field approximately read

$$\square\Phi = -Ge^{-\Phi}\mathcal{F}_{\mu\nu}\mathcal{F}^{\mu\nu} , \quad (3.18)$$

$$T_{\mu\nu}^{\text{EM}} = -g_{\mu\nu}\frac{e^{-\Phi}}{16\pi}\mathcal{F}_{\mu\nu}\mathcal{F}^{\mu\nu} + \frac{e^{-\Phi}}{4\pi}\mathcal{F}_\mu{}^\rho\mathcal{F}_{\nu\rho} . \quad (3.19)$$

Solving the equations of motion in the region outside the monopole core, we obtain

$$B_{\text{ext}}(r) = A_{\text{ext}}(r) = 1 - 8\pi G\eta^2 - \frac{2GM}{r} , \quad R(r) = \sqrt{r(r - \zeta)} , \quad (3.20)$$

$$\Phi(r) = -\ln\left[1 - \frac{\zeta}{r}\right] , \quad Q_m = \sqrt{M\zeta} , \quad (3.21)$$

where  $r \geq \zeta$ , which ensures that the geometry remains real. Here  $R(r)$  is the areal radius. The quantity  $M$  is the ADM mass of the monopole, and  $\zeta$  is the dilaton scalar charge that controls the  $\frac{1}{r}$ -term of dilaton in its expansion for large  $r$ ,

$$\Phi(r) \simeq \frac{\zeta}{r} + \mathcal{O}(r^{-2}) . \quad (3.22)$$

The magnetic charge of the monopole is denoted by  $Q_m$ , and is determined by both the dilaton scalar charge and the monopole mass, implying that the dilaton field acts as a secondary scalar hair. For a review of hairy black holes, see Ref. [54]; for studies of magnetically charged hairy black holes in non-linear electrodynamics, see Refs. [55, 56].

The solutions (3.20) and (3.21) reduce, for  $\eta = 0$ , to those first obtained in Ref. [57]. In Schwarzschild coordinates, where  $g_{\theta\theta} = R^2$ , these solutions read

$$B_{\text{ext}}(R) = 1 - 8\pi G\eta^2 - \frac{4GM}{\zeta + \sqrt{4R^2 + \zeta^2}} , \quad A_{\text{ext}}(R) = \frac{B(R)}{F(R)} , \quad (3.23)$$

$$F(R) = \frac{4R^2}{\zeta^2 + 4R^2} , \quad \Phi(R) = -\ln\left[1 - \frac{2\zeta}{\zeta + \sqrt{4R^2 + \zeta^2}}\right] . \quad (3.24)$$

Inside the monopole core ( $r < \delta$ ), the global  $O(3)$  symmetry is unbroken. We assume that the Higgs triplet vanishes in this region,  $h(r) = 0$ . In the spirit of Ref. [22], we further assume that gravity becomes strong in the core and that the underlying string theory is in a strongly coupled regime. Accordingly, the dilaton is taken to be stabilized at large values near the origin ( $\Phi \rightarrow +\infty$ ), such that  $\frac{e^{-2\Phi}}{\beta_{\text{BI}}}F_{\mu\nu}F^{\mu\nu} \approx 0$ . In this limit, the dilaton equation is trivially satisfied and the electromagnetic sector becomes negligible. Consequently, regular solutions of the Einstein equations can be obtained inside the monopole core. In Schwarzschild coordinates, where  $g_{\theta\theta} = R^2$ , the metric functions are given by

$$B_{\text{int}}(R) = A_{\text{int}}(R) = 1 - \frac{2\pi G\lambda\eta^4}{3}R^2 . \quad (3.25)$$

This solution describes a de Sitter monopole core, in agreement with similar constructions in Refs. [26, 35, 37].

To perform the Israel matching at the surface of the de Sitter core of radius  $\delta$ , and thereby determine both the ADM mass  $M$  and the core radius  $\delta$ , we adopt the approximation introduced in Ref. [26], namely a homogeneous Reissner–Nordström (RN) metric valid at large  $R$ :

$$B_{\text{ext}}(R) \approx A_{\text{ext}}(R) \approx 1 - 8\pi G\eta^2 - \frac{2GM}{R} + \frac{GM\zeta}{R^2} + \mathcal{O}\left(\frac{1}{R^3}\right). \quad (3.26)$$

The Israel matching conditions at  $R = \delta$  read

$$B_{\text{ext}}(\delta) = B_{\text{int}}(\delta), \quad B'_{\text{ext}}(\delta) = B'_{\text{int}}(\delta). \quad (3.27)$$

To simplify the analysis, we introduce the dimensionless variables  $\tilde{R} = \eta\sqrt{\lambda}R$ ,  $\tilde{\delta} = \eta\sqrt{\lambda}\delta$ ,  $\tilde{\zeta} = \eta\sqrt{\lambda}\zeta$  and  $\tilde{M} = \frac{\sqrt{\lambda}}{\eta}M$ . Substituting the approximate exterior metric (3.26) and interior metric (3.25) and using  $8\pi G = 1$  in reduced Planck units, the two conditions become respectively

$$\frac{2\tilde{M}}{\tilde{\delta}} - \frac{\tilde{M}\tilde{\zeta}}{\tilde{\delta}^2} = \frac{2\pi\tilde{\delta}^2}{3}, \quad (3.28)$$

$$\frac{2\tilde{M}}{\tilde{\delta}^2} - \frac{2\tilde{M}\tilde{\zeta}}{\tilde{\delta}^3} = \frac{4\pi\tilde{\delta}}{3}. \quad (3.29)$$

Dividing (3.28) by  $\tilde{\delta}$  and comparing with (3.29) fixes  $\tilde{M}$  in terms of  $\tilde{\delta}$  and  $\tilde{\zeta}$ . The matching conditions then yield

$$\tilde{M} = \frac{2\pi}{3} \frac{\tilde{\delta}^4}{\tilde{\zeta} - \tilde{\delta}}, \quad (3.30)$$

and three real roots for  $\tilde{\delta}$ , when  $\tilde{\zeta} \in [0, \frac{3}{2\sqrt{2}}] \cup [4\sqrt{3}, +\infty)$ :

$$\tilde{\delta}_1 = \frac{2}{9} \left( \tilde{\zeta} - \text{sign}[a]\sqrt{\tilde{\zeta}^2 + 27} \left( \cos \left[ \frac{1}{3} \tan^{-1} \left[ \frac{\sqrt{b}}{|a|} \right] \right] + \sqrt{3} \sin \left[ \frac{1}{3} \tan^{-1} \left[ \frac{\sqrt{b}}{|a|} \right] \right] \right) \right), \quad (3.31)$$

$$\tilde{\delta}_2 = \frac{2}{9} \left( \tilde{\zeta} - \text{sign}[a]\sqrt{\tilde{\zeta}^2 + 27} \left( \cos \left[ \frac{1}{3} \tan^{-1} \left[ \frac{\sqrt{b}}{|a|} \right] \right] - \sqrt{3} \sin \left[ \frac{1}{3} \tan^{-1} \left[ \frac{\sqrt{b}}{|a|} \right] \right] \right) \right), \quad (3.32)$$

$$\tilde{\delta}_3 = \frac{2}{9} \left( \tilde{\zeta} + 2\text{sign}[a]\sqrt{\tilde{\zeta}^2 + 27} \cos \left[ \frac{1}{3} \tan^{-1} \left[ \frac{\sqrt{b}}{|a|} \right] \right] \right), \quad (3.33)$$

where

$$a = 4\tilde{\zeta}^3 - 567\tilde{\zeta}, \quad b = 27^2(\tilde{\zeta}^2 - 48)(8\tilde{\zeta}^2 - 9). \quad (3.34)$$

For  $\tilde{\zeta} \in [0, \frac{3}{2\sqrt{2}}] \cup [4\sqrt{3}, +\infty)$  one finds  $b > 0$ . In the special case  $\tilde{\zeta} = 0$ , the only positive root is  $\tilde{\delta}_1 = 2$ , yielding a monopole mass  $\tilde{M} = -16\pi/3$ , which corresponds to the trivial GM solution [23]. For  $\tilde{\zeta} \in (\frac{3}{2\sqrt{2}}, 4\sqrt{3})$  the solutions are non-physical, as only a single real negative root exists:

$$\tilde{\delta} = \frac{2}{9} \left( \tilde{\zeta} - 2^{2/3} \frac{\tilde{\zeta}^2 + 27}{(-a - \sqrt{-b})^{1/3}} - 2^{-2/3} (-a - \sqrt{-b})^{1/3} \right) < 0, \quad (3.35)$$

where  $a$  and  $b$  are defined in Eq. (3.34); in this interval one has  $a, b < 0$ .

For the solution to describe a physically acceptable particle-like configuration, both the de Sitter core radius and the monopole mass must be positive. These conditions are simultaneously satisfied for  $\tilde{\zeta} \geq 4\sqrt{3}$ , where two positive roots for the dimensionless core radius  $\tilde{\delta}$  exist. Let us denote them as  $\tilde{R}_{\text{dS1}}$  and  $\tilde{R}_{\text{dS2}}$ . For  $\tilde{\zeta} \geq 4\sqrt{3}$ , they are given by

$$\tilde{R}_{\text{dS1}} = \begin{cases} \tilde{\delta}_1 & \text{if } 4\sqrt{3} \leq \tilde{\zeta} \leq \frac{9\sqrt{7}}{2} \\ \tilde{\delta}_3 & \text{if } \frac{9\sqrt{7}}{2} < \tilde{\zeta} \end{cases}, \quad (3.36)$$

$$\tilde{R}_{\text{dS2}} = \tilde{\delta}_2, \quad \tilde{\zeta} > 4\sqrt{3}. \quad (3.37)$$

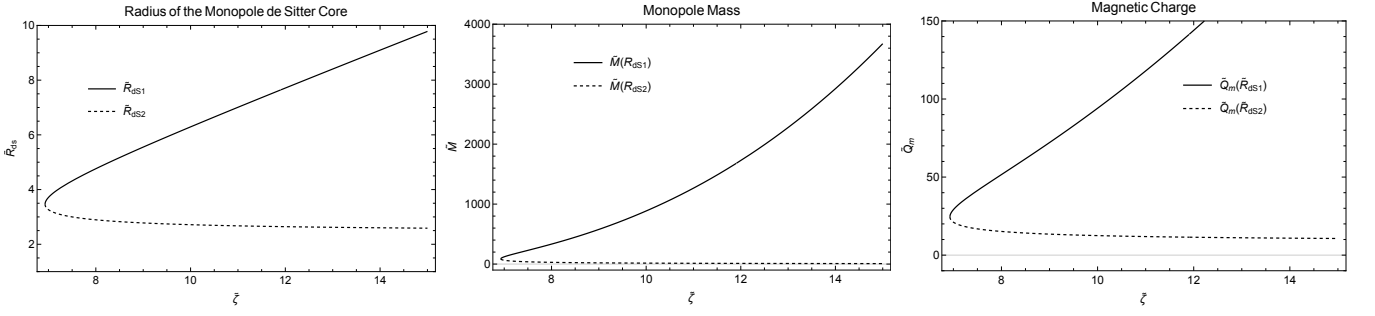


FIG. 1. Dimensionless de Sitter core radius  $\tilde{R}_{\text{dS}}$  (left), monopole mass  $\tilde{M}$  (middle), and magnetic charge  $\tilde{Q}_m$  (right) as functions of the dimensionless dilaton charge  $\tilde{\zeta}$ . Solid lines correspond to the solution branch  $\tilde{R}_{\text{dS}1}$  [Eq. (3.36)], while dashed lines correspond to  $\tilde{R}_{\text{dS}2}$  [Eq. (3.37)].

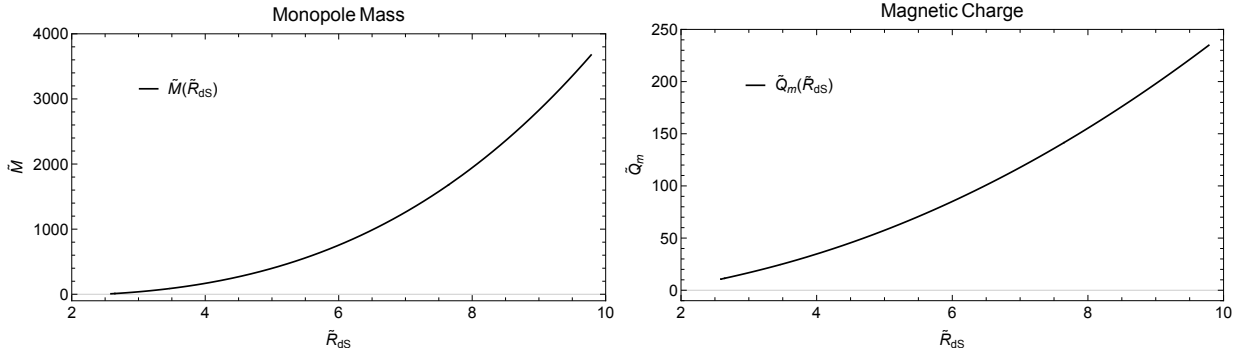


FIG. 2. Dimensionless monopole mass  $\tilde{M}$  (left) and magnetic charge  $\tilde{Q}_m$  (right) as functions of the de Sitter core radius  $\tilde{R}_{\text{dS}}$ .

These solutions satisfy  $\tilde{R}_{\text{dS}2} \in [\sqrt{6}, 2\sqrt{3}]$ ,  $\tilde{R}_{\text{dS}1} \in [2\sqrt{3}, +\infty)$ , and  $\tilde{M} \in [0, +\infty)$ .

In Fig. 1, we plot the de Sitter core radius  $R_{\text{dS}}$ , the monopole mass  $\tilde{M}$ , and the magnetic charge  $\tilde{Q}_m = \sqrt{\tilde{\zeta}\tilde{M}}$  as functions of the dilaton charge  $\tilde{\zeta}$ . In Fig. 2, the monopole mass and magnetic charge are shown as functions of the de Sitter core radius  $\tilde{R}_{\text{dS}}$ . Both  $\tilde{M}(\tilde{R}_{\text{dS}})$  and  $\tilde{Q}_m(\tilde{R}_{\text{dS}})$  are monotonically increasing functions of  $\tilde{R}_{\text{dS}}$ .

**Remark (minimum magnetic charge).** In the limiting case of the smallest monopole,  $\tilde{R}_{\text{dS}} \rightarrow \sqrt{6}$  (the lower end of the  $\tilde{R}_{\text{dS}2}$  branch), the dimensionless mass vanishes  $\tilde{M} \rightarrow 0$  while the magnetic charge  $\tilde{Q}_m = \sqrt{\tilde{\zeta}\tilde{M}}$  approaches a finite nonzero value. This implies the existence of a *minimum nonzero magnetic charge* in this model: a zero-mass limit exists in which the monopole is held up entirely by its magnetic charge and the de Sitter core pressure, with no gravitational contribution.

Having determined the monopole mass and the radius of the de Sitter core, we now assess the validity of the approximations used in the Israel matching. Outside the monopole core, in the large- $R$  region, the metric components read

$$B_{\text{ext}}(R) \approx 1 - 8\pi G\eta^2 - \frac{2GM}{R} + \frac{GM\zeta}{R^2} - \frac{GM\zeta^2}{4R^3} + \mathcal{O}\left(\frac{1}{R^5}\right), \quad (3.38)$$

$$A_{\text{ext}}(R) \approx 1 - 8\pi G\eta^2 - \frac{2GM}{R} + \frac{GM\zeta + (1 - 8\pi G\eta^2)\frac{\zeta^2}{4}}{R^2} + \mathcal{O}\left(\frac{1}{R^3}\right). \quad (3.39)$$

In deriving the analytic expressions for the monopole mass and core radius, we retained terms up to the Reissner–Nordström (RN) contribution in the metric function  $B(R)$ . To assess the validity of this approximation, we plot in the left panel of Fig. 3 the ratio of the  $R^{-3}$  and  $R^{-2}$  terms in Eq. (3.38), evaluated at  $R = \tilde{R}_{\text{dS}}$ . For small monopoles, this ratio becomes significantly larger than unity, indicating that higher-order terms cannot be neglected. For large monopoles, the ratio approaches a lower bound of  $3/8$ . Overall, the RN approximation is unreliable for small monopoles, where the mass and charge may deviate substantially from the analytic estimates; for larger monopoles, the approximation improves, although it remains approximate and may still lead to quantitative discrepancies.

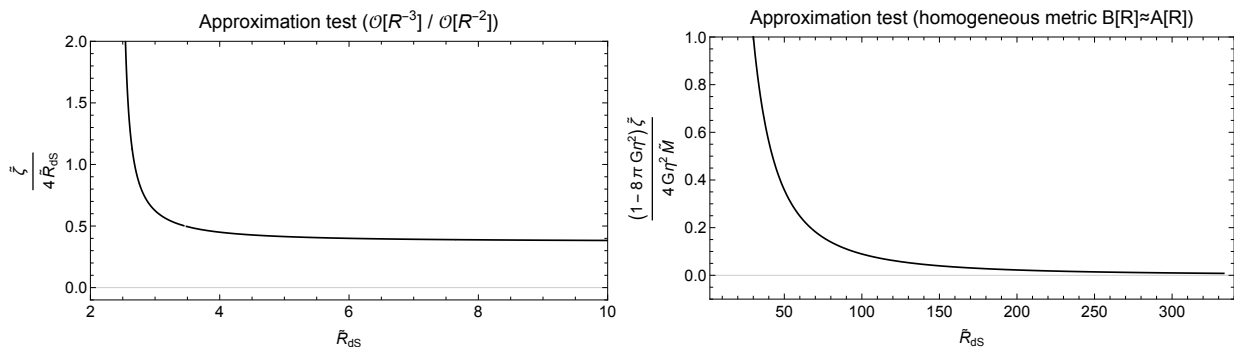


FIG. 3. Left: Ratio of the  $R^{-3}$  to  $R^{-2}$  terms in the large- $R$  expansion of the metric function  $B(R)$  in Schwarzschild coordinates [Eq. (3.38)], plotted as a function of the de Sitter core radius  $R_{\text{dS}}$ . Right: Relative difference between the Reissner–Nordström contributions to the metric functions  $B(R)$  and  $A(R)$ , defined as  $(A(R) - B(R))/B(R)$ , as a function of  $R_{\text{dS}}$ .

In addition, we assumed a homogeneous metric outside the monopole core. For this approximation to hold up to the RN order, the metric functions  $B(R)$  and  $A(R)$  must coincide up to terms of order  $R^{-2}$ , which requires  $G\tilde{M} \gg (1 - 8\pi G\eta^2) \frac{\zeta}{4\eta^2}$ . In the right panel of Fig. 3, we plot the ratio  $(1 - 8\pi G\eta^2) \frac{\zeta}{4\eta^2 G\tilde{M}}$  as a function of  $R_{\text{dS}}$ , in units  $G = 1$  and for  $\eta = 10^{-2}$ . This ratio decreases to zero as  $R_{\text{dS}} \rightarrow \infty$ , demonstrating that the homogeneous metric approximation becomes increasingly accurate for large monopoles.

Although the analytic approximations break down in part of the parameter space, in particular in the small-mass regime, we now verify numerically that magnetic monopole solutions still exist and determine their masses in cases where the analytic treatment becomes unreliable. As a representative example, we consider

$$\eta = 10^{-2}, \quad \lambda = 10^4, \quad \beta_{\text{BI}} = 1, \quad \zeta = \frac{4\sqrt{3}}{\eta\sqrt{\lambda}}, \quad (3.40)$$

and we work in units  $G = c = 1$ . The BI parameter is related to the string scale  $M_s$  via  $\beta_{\text{BI}} \approx M_s^4$ . Identifying  $M_s$  with the (reduced) Planck scale,

$$M_s \simeq M_{\text{Pl}}, \quad (3.41)$$

the BI parameter reads

$$\beta_{\text{BI}} = 1, \quad (3.42)$$

in (reduced) Planck units, where:

$$8\pi G = 1. \quad (3.43)$$

A numerical analysis of the standard GM [23] has been performed in Ref. [35], using the Runge-Kutta method. The authors of Ref. [37] also find a numerical solution of a GM associated with the spontaneous breaking of a global  $O(3)$  symmetry within an extended Gauss Bonnet theory of gravity, which includes a dilaton field. The presence of the dilaton and Higgs fields makes the numerical problem stiff, and thus certain numerical methods for solving the equations of motion can become numerically unstable unless an extremely small step size is used. We remind the reader that an ordinary differential equation problem is considered stiff if the desired solution changes slowly while nearby solutions change rapidly, necessitating small steps for the numerical method to achieve satisfactory results. This is also the case with the dilaton and Higgs fields in our work. Therefore, we will solve the differential problems exploiting the “StiffnessSwitching” method of Mathematica, which uses a pair of extrapolation methods as the default. Specifically, the stiff solver uses the Linearly Implicit Euler method, while the non-stiff solver uses the Explicit Modified Midpoint method.

The equations of motion are given by Eqs. (3.5)–(3.8). The ansatz (3.14) automatically satisfies the BI equations of motion. Additionally, the remaining five independent equations of motion yield  $W(r) = Q_m/R^2(r)$ . To ensure that the equations of motion are satisfied in the large- $r$  region, the magnetic charge must satisfy  $Q_m = \sqrt{M\zeta}$ , where  $M$  is the monopole mass and  $\zeta$  is the dilaton charge. We work in the coordinate system  $(t, r, \theta, \phi)$ , with the metric given by Eq. (3.13) and  $R(r) = \sqrt{r(r - \zeta)}$  for  $r \geq \zeta$ .

To obtain the numerical solutions, we solve the remaining four independent equations of motion for  $B'(r)$ ,  $A'(r)$ ,  $h''(r)$ , and  $\Phi''(r)$ , where the prime denotes differentiation with respect to the radial coordinate  $r$ . These equations

are solved simultaneously. We do not display their explicit form, as the resulting expressions are lengthy and not particularly illuminating.

To avoid singular behavior, we impose initial conditions at  $r = \zeta + \epsilon$  with  $\epsilon = 10^{-6}$ :

$$\begin{aligned} h'(\zeta + \epsilon) &\approx 4 \cdot 10^4, \quad h(\zeta + \epsilon) \approx h'(\zeta + \epsilon)\epsilon, \quad \Phi'(\zeta + \epsilon) \approx -10^6, \\ \Phi(\zeta + \epsilon) &\approx 13, \quad B(\zeta + \epsilon) \approx 1, \quad A(\zeta + \epsilon) \approx 10^{-2}. \end{aligned} \quad (3.44)$$

These initial conditions are chosen to reproduce the correct asymptotic behavior. They are also consistent with the expected structure inside the dS core: for the chosen coordinate system, the interior metric functions read  $B_{\text{int}}(r) = 1 - \frac{2\pi G\lambda\eta^4}{3}r(r - \zeta)$  and  $A_{\text{int}}(r) = B_{\text{int}}(r)/R'^2(r)$ , implying  $B(\zeta + \epsilon) \approx 1$  and  $A(\zeta + \epsilon) \approx 0$  near the origin. In Schwarzschild coordinates, both metric functions remain regular, ensuring the absence of curvature singularities. The Higgs field is approximately zero near the origin, where the global  $O(3)$  symmetry is unbroken, and rapidly approaches unity outside the monopole core, where the symmetry is broken. Accordingly, its radial derivative is large near the origin. The initial conditions for the dilaton are chosen to reproduce the asymptotic profile  $\Phi(r) = -\ln\left(1 - \frac{\zeta}{r}\right)$  at large  $r$ . In addition, we impose that the mass function

$$M(r) = \frac{r}{2G} (1 - 8\pi G\eta^2 - B(r)), \quad (3.45)$$

approaches a constant as  $r \rightarrow \infty$ . The asymptotic value of  $M(r)$  then corresponds to the ADM mass of the monopole.

In Fig. 4, we present the numerical solutions and compare them with the corresponding analytic results. For the chosen parameter set, the Israel matching predicts a de Sitter core radius  $r_{\text{dS}} \approx \frac{9}{\eta\sqrt{\lambda}}$ . The Higgs profile (top-left panel) increases rapidly in the vicinity of  $r_{\text{dS}}$  and approaches unity for  $r > r_{\text{dS}}$ , indicating that the global  $O(3)$  symmetry is unbroken inside the core and broken outside. This behavior is consistent with previous studies of global monopoles [35, 37]. The dilaton field (top-right panel) attains large values near the origin and reproduces the analytic large- $r$  profile given in Eq. (3.21). Deviations between the numerical and analytic solutions appear in the transition region near the monopole shell, where the approximations are not valid. The metric function  $B(r)$  (bottom-left panel) remains regular at the origin and approaches the analytic solution (3.20) outside the monopole core. The approximation based on Israel matching is also shown for comparison. The metric function  $A(r)$  (bottom-right panel) exhibits the expected asymptotic behaviour, approaching the analytic large- $r$  solution  $A_{\text{ext}}(r) = B_{\text{ext}}(r)$ . For comparison, we also display the approximate solution  $A_{\text{appr}}(r) = \frac{4r(r-\zeta)}{(2r-\zeta)^2} A(R(r))$ , where  $A(R)$  is obtained from the Israel matching. In the bottom panels of Fig. 4, the approximate solutions for the metric functions closely follow the numerical profiles.

In Fig. 5, we show the numerical mass function defined in Eq. (3.45). Outside the monopole core,  $M(r)$  follows the analytic behavior implied by the metric function  $B(r)$  in Eq. (3.20). The corresponding Reissner–Nordström approximation used in the Israel matching is also displayed for comparison. The numerical solution approaches a constant as  $r \rightarrow \infty$ , which corresponds to the ADM mass of the monopole. For  $\zeta = 4\sqrt{3}$ , the Israel matching predicts  $Q_m^{\text{Is}} \approx \frac{24}{\sqrt{\lambda}}$  and  $M^{\text{Is}} \approx 87 \frac{\eta}{\sqrt{\lambda}}$ . The numerical solution yields  $Q_m \approx \sqrt{2} Q_m^{\text{Is}}$  and  $M \approx 2 M^{\text{Is}}$ . Thus, the numerical results confirm the existence of magnetic monopole solutions and show that the analytic estimates capture the correct order of magnitude for both the mass and the magnetic charge.

Finally, whereas the self-energy of a monopole diverges in standard Maxwell electrodynamics, it remains finite in Born–Infeld electrodynamics. To illustrate this, we work in Schwarzschild coordinates with  $R(r) = r$  for  $r \geq 0$ . In Maxwell theory, the Lagrangian density behaves as  $-\mathcal{F}_{\mu\nu}\mathcal{F}^{\mu\nu} = -\frac{2Q_m^2}{r^4}$ , which leads to a divergent energy density near the origin and hence an infinite self-energy. By contrast, in the BI case, the Lagrangian density near the origin scales as  $\mathcal{L}_{\text{BI}} \approx -\frac{\sqrt{\beta_{\text{BI}}}}{4\sqrt{2}\pi} \sqrt{\mathcal{F}_{\mu\nu}\mathcal{F}^{\mu\nu}} = -\frac{\sqrt{\beta_{\text{BI}}}}{4\pi} \frac{Q_m}{r^2}$ . The self-energy in this region is obtained by integrating the Hamiltonian density over the small-radius volume, behaves as  $E_{\text{BI}}(r \ll 1) = Q_m \sqrt{\beta_{\text{BI}}} \int dr$ , and is therefore finite. Furthermore, integrating the Hamiltonian density over the entire space, using the parameter set adopted in the numerical analysis and the numerical dilaton profile  $\Phi(r)$ , yields a total monopole self-energy  $E_{\text{BI}} \approx 0.7$ , confirming the finiteness of the solution.

To summarise, the global monopole model with dilaton and Born–Infeld interactions admits self-gravitating magnetic monopole solutions with positive ADM mass, where the magnetic charge is not an independent parameter but is tied to the dilaton charge and the monopole mass. The approximate analytic construction, based on a de Sitter core matched to an exterior magnetically charged geometry, captures the main qualitative features of the solution and identifies the parameter regime in which physically acceptable monopoles exist. Although the Israel matching and Reissner–Nordström-type approximation are not uniformly accurate across the full parameter space, the numerical analysis confirms the existence of the solutions and shows that the predicted masses and magnetic charges are correct at the level of order of magnitude. An additional appealing feature of the model is that the Born–Infeld sector renders

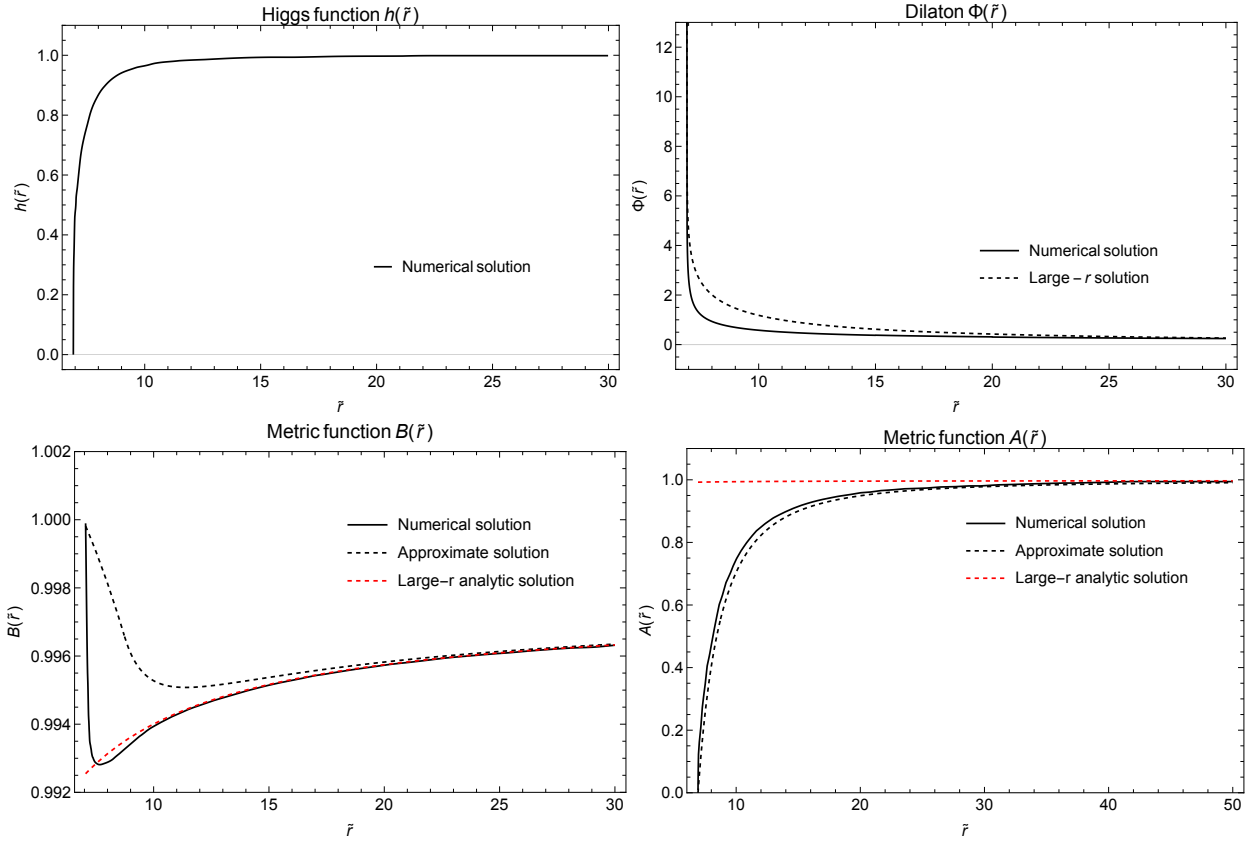


FIG. 4. Numerical solutions of the equations of motion. Top-left: Higgs function. Top-right: Dilaton field (numerical solution shown by the solid line, analytic large- $r$  solution by the dashed line). Bottom panels: Metric functions  $B(\tilde{r})$  (left) and  $A(\tilde{r})$  (right), including the numerical solutions (solid black), the Israel-matching approximations (dashed black), and the analytic large- $r$  solutions (dashed red).

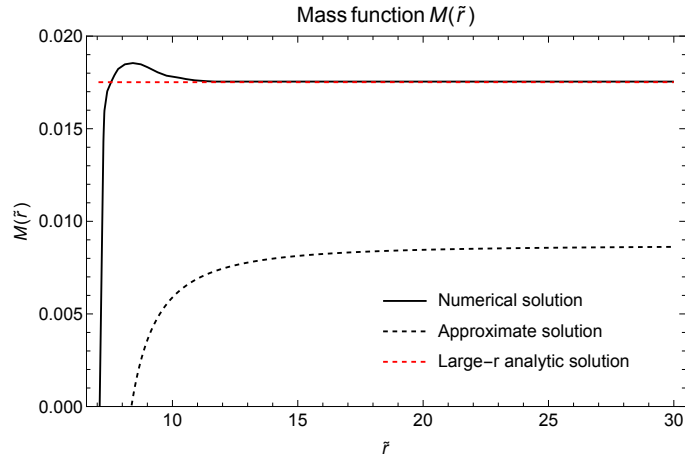


FIG. 5. Mass function  $M(\tilde{r})$  as a function of the dimensionless radius  $\tilde{r}$ . The numerical solution (solid black), the Israel-matching approximation (dashed black), and the analytic large- $r$  solution (dashed red) are shown. The mass function approaches a constant value—the ADM mass of the monopole—at large  $r$ . The numerical and approximate predictions for the monopole mass differ by approximately a factor of two.

the monopole self-energy finite, in contrast to the Maxwell case. Altogether, these results support the picture that string-inspired dilaton and Born–Infeld couplings provide a natural framework in which global monopoles can be promoted to physically viable magnetic monopoles.

#### IV. DYONS FROM GLOBAL MONOPOLES WITH DILATON AND AXION CHARGES

In this section we extend the previous construction by incorporating a Kalb–Ramond (KR) field, whose four-dimensional dual description introduces an axion degree of freedom. This additional sector naturally arises in string-inspired frameworks and leads to a non-trivial coupling between the axion and the electromagnetic field through the topological term  $\mathcal{F}\tilde{\mathcal{F}}$ . As a result, the system admits configurations carrying both electric and magnetic charges, i.e. dyonic solutions. Our aim is to investigate whether global monopoles coupled to gravity, a dilaton, and a KR axion field can give rise to self-gravitating dyon solutions with well-defined ADM mass and finite self-energy. We first formulate the effective action and corresponding equations of motion, and then construct static, spherically symmetric solutions by analyzing separately the large- and small-radius regimes, following the approach developed in the previous section.

In addition to the model of the previous section, we introduce a Kalb–Ramond (KR) field with dynamics described by the following Lagrangian

$$\mathcal{L}^{\text{KR}} = \frac{\sqrt{-g}}{16\pi G} \left( \frac{e^{-2\Phi}}{6} H^{\rho\mu\nu} H_{\rho\mu\nu} \right), \quad (4.1)$$

where  $H_{\rho\mu\nu}$  is the KR field strength tensor, which is associated with the KR field  $\mathcal{B}_{\mu\nu}$  via  $H_{\rho\mu\nu} = \partial_\rho \mathcal{B}_{\mu\nu} + \partial_\mu \mathcal{B}_{\nu\rho} + \partial_\nu \mathcal{B}_{\rho\mu}$ . The KR field satisfies the following equations of motion

$$\nabla_\rho (e^{-2\Phi} H^{\rho\mu\nu}) = 0, \quad (4.2)$$

and the Bianchi identity  $\varepsilon^{\mu\nu\rho\sigma} \nabla_\sigma H_{\mu\nu\rho} = 0$ . In 4-dimensions the KR field strength is dual to an axion field  $b$

$$H_{\mu\nu\rho} = e^{2\Phi} \varepsilon_{\mu\nu\rho}{}^\sigma \partial_\sigma b. \quad (4.3)$$

In superstring theory, anomaly cancellation requires a modification of the KR field strength by appropriate gauge and Lorentz Chern-Simons terms. Thus, as discussed in [21], the Bianchi identity is modified as

$$\varepsilon^{\mu\nu\rho\sigma} \nabla_\sigma H_{\mu\nu\rho} = \frac{1}{16\pi} (R_{\mu\nu\rho\sigma} \tilde{R}^{\mu\nu\rho\sigma} - \mathcal{F}_{\mu\nu} \tilde{\mathcal{F}}^{\mu\nu}). \quad (4.4)$$

The KR field strength given in Eq. (4.3) identically satisfies the KR equations of motion (4.2). The complete action incorporating the dynamics of the axion field reads

$$S = \int d^4x \sqrt{-g} \left[ \frac{R}{16\pi G} + \mathcal{L}_{\text{GM}} - \frac{1}{32\pi G} \nabla^\mu \Phi \nabla_\mu \Phi + \frac{1}{16\pi} \mathcal{L}_{\text{BI}} - \frac{e^{2\Phi}}{32\pi G} \nabla_\mu b \nabla^\mu b + \frac{b}{16\pi G} (R_{\mu\nu\rho\sigma} \tilde{R}^{\mu\nu\rho\sigma} - \mathcal{F}_{\mu\nu} \tilde{\mathcal{F}}^{\mu\nu}) \right]. \quad (4.5)$$

The equation of motion of the KR axion field associated with this action coincides with the Bianchi identity given by Eq. (4.4) and reads

$$\square b = R_{\mu\nu\rho\sigma} \tilde{R}^{\mu\nu\rho\sigma} - \mathcal{F}_{\mu\nu} \tilde{\mathcal{F}}^{\mu\nu}. \quad (4.6)$$

To construct a static, spherically symmetric solution with both electric and magnetic charges, we consider that the axion depends only on the radial coordinate  $b = b(r)$ . For static and spherically symmetric spacetimes one has  $R_{\mu\nu\rho\sigma} \tilde{R}^{\mu\nu\rho\sigma} = 0$ , while in the presence of both electric and magnetic fields  $\mathcal{F}_{\mu\nu} \tilde{\mathcal{F}}^{\mu\nu} \neq 0$ . We further impose a monopole configuration analogous to that of the previous section, and therefore divide the analysis into large- and small- $r$  regimes. In the large- $r$  region, where the global  $O(3)$  symmetry is broken, we assume that the BI electrostatics coincide with the standard Maxwell electrostatics, and the EM field equations read

$$\nabla_\mu (e^{-\Phi} \mathcal{F}^{\mu\nu} + b \tilde{\mathcal{F}}^{\mu\nu}) = 0, \quad (4.7)$$

which is identically satisfied, as shown in [58], by considering the following non-vanishing components of the EM field strength

$$\mathcal{F}_{\theta\phi} = -\mathcal{F}_{\phi\theta} = Q_m \sin\theta \quad \text{and} \quad \mathcal{F}_{tr} = -\mathcal{F}_{rt} = e^{\Phi(r)} \frac{Q_e - (b(r) - b_0)Q_m}{R^2(r)}, \quad (4.8)$$

where  $Q_e$  and  $Q_m$  are the electric and magnetic charges of the dyon respectively, and  $b_0$  is the asymptotic value for the axion field at spatial infinity. The combination

$$Q_e^{\text{eff}}(r) := Q_e - (b(r) - b_0)Q_m, \quad (4.9)$$

appearing in (4.8), defines an effective electric charge: it vanishes in the purely magnetic limit, either when  $Q_e = 0$  and  $b(r) = b_0$ , or more generally when the axion dressing exactly compensates the bare electric charge.

For the metric ansatz in Eq. (3.13) the equations of motion are solved by

$$B_{\text{ext}}(r) = A_{\text{ext}}(r) = 1 - 8\pi G\eta^2 - \frac{2GM}{r}, \quad R(r) = \sqrt{r(r - \zeta)}, \quad (4.10)$$

$$\Phi(r) = -\ln \left[ \frac{Q^2 R^2(r)}{Q^2 r^2 - Q_e^2 \zeta (2r - \zeta)} \right], \quad b(r) = b_0 + \frac{\zeta Q_e Q_m (2r - \zeta)}{(r - \zeta)^2 Q_e^2 + r^2 Q_m^2}, \quad (4.11)$$

where  $r > \zeta$ ,  $M$  is the monopole mass, and

$$Q^2 = Q_e^2 + Q_m^2 = M\zeta. \quad (4.12)$$

The above solution generalizes the magnetic monopole case of the previous section, with the replacement  $Q_m \rightarrow Q = \sqrt{Q_e^2 + Q_m^2}$ .

In the small- $r$  region, the interior solution coincides with that of the previous section, as long as the dilaton is stabilized at a very large value and the axion is zero inside the monopole core. Thus, we fix  $b_0 = -\frac{Q_e}{Q_m}$  in order to obtain  $b(\zeta) = 0$ , and the solution inside the monopole core is given by Eq. (3.25). The process of the Israel matching at the monopole core and the numerical calculations are similar to those performed in the previous section, as long as we replace  $Q_m$  with  $Q$ , and hence they are omitted.

In summary, the inclusion of the Kalb–Ramond axion field leads to dyonic generalizations of the global monopole solutions studied previously. The axion coupling induces an effective electric charge through its interaction with the electromagnetic sector, resulting in a non-trivial dressing of the electric component of the field strength. The resulting solutions are characterized by a combined charge  $Q^2 = Q_e^2 + Q_m^2$ , which enters the geometry in a manner analogous to the purely magnetic case, while the axion field interpolates between distinct asymptotic values and vanishes inside the monopole core. The interior solution remains unchanged under appropriate boundary conditions, and the matching procedure is analogous to the monopole case. Overall, these results demonstrate that the framework naturally accommodates self-gravitating dyon solutions, with the axion field playing a central role in relating the electric charge to the underlying topological and scalar structure of the system.

## V. STABILITY ANALYSIS OF THE SOLUTIONS

We next discuss the stability of the MM and Dyon solutions. We examine two types of stability. Mechanical one, and dynamical stability, under linearized perturbations of the solution (linear stability). We commence the analysis by examining mechanical stability criteria and the satisfaction of energy conditions of the self-gravitating solutions.

### A. Mechanical Stability Criteria and Energy Theorems

In this section, we analyze the mechanical stability of the magnetic monopole and dyon solutions obtained in the previous sections and examine the associated energy conditions. These provide important diagnostics of the physical viability of the solutions, exploring the behaviour of the stress–energy tensor and ensuring the absence of pathologies such as negative energy densities or instabilities.

To define and perform the mechanical stability tests and examine the energy conditions, we write the stress-energy tensor in the physical coordinate system  $(t, R, \theta, \varphi)$  in the form of an anisotropic fluid:

$$T^{\mu\nu} = (\rho_E + p_\theta)u^\mu u^\nu + (p_R - p_\theta)n^\mu n^\nu + p_\theta g^{\mu\nu}, \quad (5.1)$$

where  $\rho_E$  denotes the energy density of the fluid measured by a comoving observer,  $p_R$  the radial pressure, and  $p_\theta$  the tangential pressure. The vector  $u^\mu$  is the timelike four-velocity of the fluid, while  $n^\mu$  is a spacelike unit vector orthogonal to  $u^\mu$  and to the angular directions. These vectors satisfy

$$u^\mu = u(R) \delta^\mu_0, \quad u^\mu u^\nu g_{\mu\nu} = -1, \quad (5.2)$$

$$n^\mu = n(R) \delta^\mu_1, \quad n^\mu n^\nu g_{\mu\nu} = 1. \quad (5.3)$$

Using Eqs. (3.9)–(3.13) and (5.1)–(5.3), one finds

$$\rho_E = -T^t_t, \quad p_R = T^R_R, \quad p_\theta = T^\theta_\theta. \quad (5.4)$$

For an anisotropic fluid of the form (5.1), the energy conditions are given by

- Null Energy Conditions (NEC):  $\rho_E + p_R \geq 0$  &  $\rho_E + p_\theta \geq 0$ ,
- Weak Energy Conditions (WEC): NEC &  $\rho_E \geq 0$ ,
- Strong Energy Conditions (SEC): NEC &  $\rho_E + p_R + 2p_\theta \geq 0$ .

Regarding the mechanical stability criteria, following Ref. [27], we examine some generalized local Laue stability conditions. The Laue condition [28] stands that, in the case of an object with a core, the exterior and interior forces should be in balance, or in other words the spatial integral of the fluid pressure  $p(R)$  in the entire space should be zero

$$\int_0^\infty dR R^2 p(R) = 0. \quad (5.5)$$

To introduce a stronger mechanical stability criterion, the authors of Ref. [27] discriminate the stress-energy tensor in two parts, one corresponding to long range (LR) force components (EM field) and one corresponding to short range (SR) contributions (the rest of the fields). Thus, the LR and SR pressures can be defined as follows

$$p_R^{\text{LR}} = T^{\text{EM}R}_R, \quad p_\theta^{\text{LR}} = T^{\text{EM}\theta}_\theta \quad (5.6)$$

and

$$p_R^{\text{SR}} = T^R_R - T^{\text{EM}R}_R, \quad p_\theta^{\text{SR}} = T^\theta_\theta - T^{\text{EM}\theta}_\theta. \quad (5.7)$$

Given these definitions for the pressures, the conservation law  $\nabla_\mu T^{\mu r} = 0$  implies

$$\frac{dp_R^{\text{SR}}}{dR} + \frac{2}{R} (p_R^{\text{SR}} - p_\theta^{\text{SR}}) = \frac{p_{\text{ext}}(R)}{R}, \quad (5.8)$$

where  $p_{\text{ext}}(R)$  is given by

$$p_{\text{ext}}(R) = -R \left( \frac{dp_R^{\text{LR}}}{dR} + \frac{2}{R} (p_R^{\text{LR}} - p_\theta^{\text{LR}}) \right). \quad (5.9)$$

The external pressure is defined in Ref. [27] as follows

$$P_{\text{ext}}(R) = \frac{1}{R^2} \int_R^\infty dr' r' p_{\text{ext}}(r'), \quad (5.10)$$

whereas the total radial force  $\mathcal{F}_{R \text{ total}}(r)$  is given by

$$\mathcal{F}_{R \text{ total}}^{\text{SR}}(R) = 4\pi R^2 [p_R^{\text{SR}}(R) + P_{\text{ext}}(R)], \quad (5.11)$$

and the other two components of the force are given by

$$\mathcal{F}_\theta^{\text{SR}}(\theta) = 2\pi \sin \theta \int_0^\infty dr' r' p_\theta^{\text{SR}}(r'), \quad (5.12)$$

and

$$\mathcal{F}_\phi^{\text{SR}} = \pi \int_0^\infty dr' r' p_\theta^{\text{SR}}(r'). \quad (5.13)$$

Stronger mechanical stability criteria than Laue condition are introduced in Ref. [27], according which the total radial force  $\mathcal{F}_{R \text{ total}}^{\text{SR}}$  should be positive at radii  $R$  close to and inside the monopole core to avoid the collapse of the soliton configurations, while the azimuthal and polar forces should be finite to avoid angular instabilities.

In the following paragraphs, we examine whether the self-gravitating magnetic monopole and dyon configurations obtained in Sections III and IV, respectively, satisfy the energy conditions and the local mechanical stability criteria.

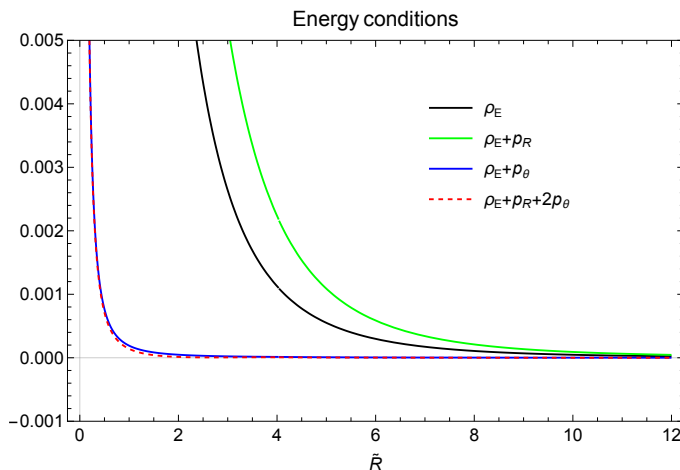


FIG. 6. Energy conditions for the numerical magnetic monopole solution with a dilaton charge (Sec. III), shown as functions of the dimensionless radius  $\tilde{R}$  for  $\eta = 10^{-2}$ ,  $\lambda = 10^4$ ,  $\beta_{\text{BI}} = 1$ , and  $\zeta = 4\sqrt{3}$ .

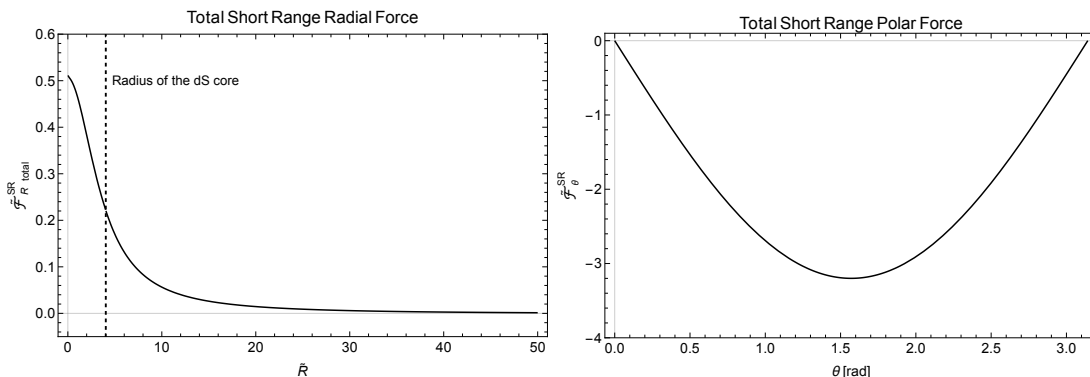


FIG. 7. Dimensionless total SR radial (left) and polar (right) forces as functions of the dimensionless radius  $\tilde{R}$  and the polar angle  $\theta$ , respectively, for the numerical magnetic monopole solution obtained in Sec. III for  $\eta = 10^{-2}$ ,  $\lambda = 10^4$ ,  $\beta_{\text{BI}} = 1$ , and  $\zeta = 4\sqrt{3}$ .

### 1. Energy conditions and mechanical stability for Magnetic Monopoles

To examine the physical consistency of the magnetic monopole solutions obtained in Sec. III, we check whether they satisfy standard energy conditions. In Fig. 6, the quantities  $\rho_E$ ,  $\rho_E + p_R$ ,  $\rho_E + p_\theta$ , and  $\rho_E + p_R + 2p_\theta$  are plotted as functions of the dimensionless radius  $\tilde{R}$ , using the numerical magnetic monopole solution of Sec. III. As illustrated in Fig. 6, all these quantities remain positive throughout spacetime, indicating that all energy conditions are satisfied. These results are consistent with the absence of curvature singularities and event horizons established earlier, as well as further support the physical consistency of the solutions, indicating that the monopole configurations satisfy standard energy requirements while remaining free of singularities and horizons.

In Fig. 7, we plot the dimensionless total SR radial force  $\tilde{\mathcal{F}}_{R\text{total}}^{\text{SR}}$ , defined in Eq. (5.11), and the total SR polar force  $\tilde{\mathcal{F}}_\theta^{\text{SR}}$ , defined in Eq. (5.12), in the left and right panels, respectively, as functions of the dimensionless radius  $\tilde{R}$  and the polar angle  $\theta$  for the numerical magnetic monopole solution obtained in Section III. The total SR radial force remains positive both inside and outside the dS core of the monopole, implying that it points outwards and therefore prevents the monopole from collapsing. Consequently, the first mechanical stability condition,  $\tilde{\mathcal{F}}_{R\text{total}}^{\text{SR}} > 0$ , is satisfied. Furthermore, the polar force remains finite, and therefore the azimuthal force, given by Eq. (5.13), is also finite. As a result, no angular instabilities arise, and the angular mechanical stability criteria are likewise satisfied.

At very large radii ( $\tilde{R} \rightarrow \infty$ ), the total SR radial force approaches the small negative value  $\tilde{\mathcal{F}}_{R\text{total}}^{\text{SR}} \rightarrow -4\pi\eta^2$ . Hence, the force becomes negative far away from the monopole, in the region where the deficit solid angle contribution proportional to  $\eta^2$  dominates. Nevertheless, this does not indicate a mechanical instability of the monopole configuration, since the radial SR force remains outward-directed within and near the monopole core.

## 2. Energy conditions and mechanical stability for Dyons

This subsection extends the purely magnetic analysis of Section V A to the dyonic solutions discussed in Section IV. We give explicit expressions for the energy–momentum components, verify the standard energy conditions, and check local force balance and shell stresses.

For the exterior dyonic background (Eq. (4.8)) the Born-Infeld (BI) electromagnetic stress tensor is

$$T^\mu{}_\nu = \frac{e^\Phi}{4\pi} \left[ \beta_{\text{BI}}(1 - \sqrt{\Delta})\delta^\mu{}_\nu + \frac{e^{-2\Phi} F^{\mu\rho} F_{\nu\rho} - \frac{e^{-4\Phi}}{2\beta_{\text{BI}}^2} (F F^*) F^{\mu\rho} F^*{}_{\nu\rho}}{\sqrt{\Delta}} \right], \quad \Delta = 1 + \frac{e^{-2\Phi} X}{2\beta_{\text{BI}}^2} - \frac{e^{-4\Phi} Y^2}{16\beta_{\text{BI}}^4}. \quad (5.14)$$

Here

$$X = F^2 = -\frac{2(Q_m^2 + Q_e^{\text{eff}2})}{R^4}, \quad Y = F F^* = -\frac{4Q_m Q_e^{\text{eff}}}{R^4}, \quad Q_e^{\text{eff}}(r) = Q_e - (b - b_0)Q_m, \quad Q^2 = Q_m^2 + Q_e^2. \quad (5.15)$$

This yields the anisotropic fluid variables

$$\rho_E = \frac{e^\Phi}{4\pi} \left[ \sqrt{\beta_{\text{BI}}^2 + e^{-2\Phi} Q^2 / R^4} - \beta_{\text{BI}} \right], \quad (5.16a)$$

$$p_R = \rho_E - \frac{e^{-\Phi} Q^2}{4\pi R^4 \sqrt{\beta_{\text{BI}}^2 + e^{-2\Phi} Q^2 / R^4}}, \quad (5.16b)$$

$$p_\theta = p_\varphi = \rho_E + \frac{e^{-\Phi} (Q_m^2 - Q_e^{\text{eff}2})}{4\pi R^4 \sqrt{\beta_{\text{BI}}^2 + e^{-2\Phi} Q^2 / R^4}}. \quad (5.16c)$$

### Energy conditions

- **NEC / WEC:** Since  $\rho_E > 0$  and  $\rho_E + p_R > 0$  by Eqs. (5.16), while  $|Q_e^{\text{eff}}| \leq Q$  guarantees  $\rho_E + p_\theta > 0$ , the null and weak energy conditions are obeyed.
- **SEC:** Adding pressures,  $\rho_E + p_R + 2p_\theta > 0$  for all  $r \geq R_{\text{core}}$ , so the strong energy condition also holds.

A numerical scan over  $0 \leq Q_e/Q_m \leq 1$ ,  $\tilde{\zeta} \geq 4\sqrt{3}$  and  $\beta_{\text{BI}} \gtrsim 100 \text{ GeV}$  can confirm that the minimum of  $\rho_E + p_\theta$  stays positive.

### Mechanical stability

The effective electric charge of the dyonic solution does not qualitatively alter the properties of the EM stress-energy tensor, while the Kalb–Ramond axion field  $b$  contributes positively to the total radial pressure of the anisotropic fluid. In addition, the axion field vanishes at the origin. Consequently, the contributions of the axion field and the effective electric charge to the total SR radial, polar, and azimuthal forces do not qualitatively modify their behavior. Therefore, the dyonic solution also satisfies the mechanical stability conditions discussed for the magnetic monopole solution.

### Summary

To summarize, the Born–Infeld dyon satisfies the energy conditions and is mechanically stable precisely within the parameter region that yields a positive ADM mass and linear perturbative stability, the latter of which is discussed in the following sections. In Appendix B, we further demonstrate that the Laue equilibrium condition is satisfied and that the shell stresses at the surface of the monopole  $dS$  core are positive, thereby providing additional confirmation of the stability of our solutions.

## B. Linear Dynamical Stability: Formalism

We now apply the GV linear dynamical stability analysis [30] to the Born–Infeld-regularised monopole model (4.5). The analysis complements the mechanical stability study above and provides an independent check of stability.

We work with static and spherically symmetric background geometries of the form (3.13). Outside the monopole core the analytic exterior solution (3.20), (3.21) is valid. For the dyon, the axion field is non-trivial in the exterior and the field strength acquires an electric component given in (4.8).

The full solution is constructed in a piecewise manner. Inside the core ( $r < \delta$ ) the Higgs field has not reached its symmetry-breaking vacuum, and the energy density is dominated by the approximately constant potential  $V \approx \lambda\eta^4/4$ , which acts as a positive cosmological constant. The interior metric is therefore approximated by de Sitter space,

$$A_{\text{int}} = B_{\text{int}} = 1 - \frac{2\pi G\lambda\eta^4}{3}r^2. \quad (5.17)$$

The shell radius  $\delta$  and the mass  $M$  are fixed by the Israel matching conditions at  $r = \delta$ , as derived in detail in the previous sections; positive ADM mass requires  $\zeta > 4\sqrt{3}$  in the dimensionless notation of Section III. For the stability analysis we focus on the exterior region  $r > \delta$ , where the interior acts as a regular inner boundary condition. Since the interior operator (a Schrödinger operator with positive centrifugal barrier  $\ell(\ell+1)/r^2$  plus the de Sitter curvature contribution  $m_{\text{eff}}^2 = 2\Lambda_{\text{eff}}/3 > 0$ ) is positive definite, any unstable mode must arise from the exterior, and the interior simply imposes regularity at  $r = 0$ .

A naive perturbation of the vector potential  $\delta A_\mu$  is not gauge invariant and mixes physical degrees of freedom with pure gauge artefacts. We therefore work throughout with gauge-invariant combinations, following the GV strategy [30]. Writing the background metric in  $2+2$  form,

$$ds^2 = g_{ab}(x) dx^a dx^b + R^2(x) \gamma_{AB} d\theta^A d\theta^B, \quad (5.18)$$

and decomposing the perturbation of the vector potential in scalar and vector spherical harmonics,

$$\delta A_a = u_a(t, r) Y_{\ell m}(\theta, \varphi), \quad (5.19)$$

$$\delta A_A = u^{(e)}(t, r) \hat{D}_A Y_{\ell m} + u^{(o)}(t, r) \hat{S}_A, \quad (5.20)$$

the gauge-invariant combinations are

$$\boxed{E_a := u_a - \partial_a u^{(e)}, \quad B := u^{(o)}}. \quad (5.21)$$

The perturbation of the field strength in mixed components is then manifestly gauge invariant:

$$\delta F_{aA} = E_a \hat{D}_A Y_{\ell m} + (\nabla_a B) \hat{S}_A. \quad (5.22)$$

The constraint  $\nabla_a(R^2 E^a) = 0$  contains no second time derivative and describes no independent propagating degree of freedom; one solves it by introducing an even-parity master field  $\Psi_e$  such that  $R^2 E^a = \epsilon^{ab} \nabla_b \Psi_e$ .

To extract the two physical propagating polarisations we introduce a null tetrad adapted to the background,

$$\{\ell^\mu, n^\mu, m^\mu, \bar{m}^\mu\}, \quad \ell \cdot n = -1, \quad m \cdot \bar{m} = +1, \quad (5.23)$$

with  $\ell^\mu$  and  $n^\mu$  null in the  $(t, r)$  plane. The two transverse propagating modes are

$$\psi_+ := \ell^a m^A \delta F_{aA}, \quad \psi_- := \ell^a \bar{m}^A \delta F_{aA}, \quad (5.24)$$

and, using the standard spin-weighted harmonic projections, one obtains

$$\psi_+ = -\frac{\sqrt{\ell(\ell+1)}}{\sqrt{2}R} \ell^a (E_a + i\nabla_a B)_{+1} Y_{\ell m}, \quad (5.25)$$

$$\psi_- = +\frac{\sqrt{\ell(\ell+1)}}{\sqrt{2}R} \ell^a (E_a - i\nabla_a B)_{-1} Y_{\ell m}. \quad (5.26)$$

These are the circularly polarised combinations of the gauge-invariant amplitudes, and are themselves gauge invariant. The full derivation of the projected radial potentials is given in Appendix A.

The electromagnetic sector is characterised by the Lagrangian  $\mathcal{L} = \mathcal{L}_{\text{BI}} + \mathcal{L}_{bF\bar{F}}$ . The excitation tensor  $P^{\mu\nu} := -2\partial\mathcal{L}/\partial F_{\mu\nu}$  satisfies  $\nabla_\mu P^{\mu\nu} = 0$ , and expanding around a background  $\bar{F}_{\mu\nu}$  gives the linearised constitutive relation

$$\delta P^{\mu\nu} = \chi^{\mu\nu}{}_{\rho\sigma} \delta F^{\rho\sigma}, \quad (5.27)$$

where  $\chi_{\mu\nu\rho\sigma} = -\frac{2\partial^2\mathcal{L}}{\partial\bar{F}^{\mu\nu}\partial\bar{F}^{\rho\sigma}}$  is the constitutive tensor evaluated on the background. In Born–Infeld–dilaton–axion theory it depends non-trivially on  $\bar{F}_{\mu\nu}$ ,  $\Phi(r)$ , and  $b(r)$ , encoding the response of the nonlinear medium.

The linearised field equation is

$$\nabla_\mu(\chi^{\mu\nu}{}_{\rho\sigma} \delta F^{\rho\sigma}) = 0, \quad (5.28)$$

supplemented by the Bianchi identity  $\nabla_{[\mu}\delta F_{\nu\rho]} = 0$ .

Substituting the helicity variables (5.25), (5.26) into the linearised field equation (5.28), performing the time-harmonic separation  $\psi_\pm(t, r) \propto e^{-i\omega t}\psi_\pm(r)$ , the standard procedure of introducing the tortoise coordinate

$$\frac{dr_*}{dr} = \frac{1}{\sqrt{A(r)B(r)}}, \quad (5.29)$$

and eliminating first radial-derivative terms, yields the Schrödinger-like system

$$\boxed{-\frac{d^2}{dr_*^2} \begin{pmatrix} \psi_+ \\ \psi_- \end{pmatrix} + \mathbf{V}(r) \begin{pmatrix} \psi_+ \\ \psi_- \end{pmatrix} = \omega^2 \begin{pmatrix} \psi_+ \\ \psi_- \end{pmatrix}}, \quad (5.30)$$

with the potential matrix

$$\mathbf{V}(r) = \begin{pmatrix} V_+(r) & \mathbb{W}(r) \\ \mathbb{W}(r) & V_-(r) \end{pmatrix}. \quad (5.31)$$

The quadratic action for the perturbations takes the form

$$S^{(2)} \sim \int dr_* \Psi^\dagger \mathcal{W}(r) \left[ -\frac{d^2}{dr_*^2} + \mathbf{V}(r) \right] \Psi, \quad (5.32)$$

where  $\mathcal{W}(r) \propto \kappa_\perp(r) \mathbf{1}$  is the weight matrix determined by the constitutive tensor. Since  $\bar{L}_X(r) = -\bar{\Delta}(r)^{-1/2}$  with  $\bar{\Delta}(r) > 0$  everywhere (the BI discriminant condition is satisfied for all solutions considered here), and the geometric prefactors  $R^2(r) > 0$  and  $\sqrt{A(r)B(r)} > 0$  hold in the exterior,  $\mathcal{W}(r)$  is positive definite throughout. The inner product

$$\langle \Psi_1, \Psi_2 \rangle = \int dr_* \Psi_1^\dagger \mathcal{W}(r) \Psi_2 \quad (5.33)$$

makes the operator  $\mathcal{O} = -d^2/dr_*^2 + \mathbf{V}(r)$  self-adjoint whenever  $\mathbf{V}(r)$  is real and symmetric and  $\mathcal{W}(r)$  is positive definite. For static backgrounds with real field profiles—as holds for both the monopole and dyonic solutions—all entries of  $\mathbf{V}(r)$  are real, and spherical symmetry implies  $V_+(r) = V_-(r) \equiv V_0(r)$ . The spectrum  $\{\omega^2\}$  is therefore entirely real, and exponential growth is impossible.

### C. Linear Stability Analysis of Monopole and Dyon

We now specialise the formalism to the two explicit solutions.

#### 1. Magnetic monopole: decoupled helicities and positive potential

For the purely magnetic monopole the only non-zero background field-strength component is  $\bar{F}_{\theta\varphi} = Q_m \sin\theta$ , so the pseudoscalar invariant vanishes identically on the background:

$$\bar{Y} = \bar{F}_{\mu\nu} \bar{\tilde{F}}^{\mu\nu} = 0.$$

Since the off-diagonal term  $\mathbb{W}(r)$  in (5.31) originates from the  $Y$ -dependent part of  $\chi^{\mu\nu}{}_{\rho\sigma}$ , it vanishes:

$$\mathbb{W}(r) = 0 \quad (\text{magnetic monopole}). \quad (5.34)$$

The two helicity sectors decouple and each satisfies an independent Regge–Wheeler-type equation,

$$-\frac{d^2\psi}{dr_*^2} + V_0(r)\psi = \omega^2\psi, \quad (5.35)$$

where  $\psi$  stands for either  $\psi_+$  or  $\psi_-$ .

In the exterior region the dilaton profile is  $\Phi(r) = -\ln(1 - \zeta/r)$ , the areal radius is  $R(r) = \sqrt{r(r - \zeta)}$ , and the metric function is  $A = B = 1 - 8\pi G\eta^2 - 2GM/r$ . The effective potential takes the form

$$V_0(r) = A(r) \left[ \frac{\ell(\ell + 1)}{R^2(r)} + \frac{V_{\text{BI}}(r) + V_{\text{dil}}(r)}{R^2(r)} \right], \quad (5.36)$$

where  $V_{\text{BI}}(r)$  contains the Born–Infeld nonlinearity corrections and  $V_{\text{dil}}(r)$  encodes the dilaton coupling. Near the core ( $r \rightarrow \zeta^+$ ), since  $R^2(r) = r(r - \zeta) \sim \zeta(r - \zeta) \rightarrow 0$  while  $A(r)$  remains finite and positive, the angular-momentum barrier dominates and one obtains

$$V_0(r) \sim \frac{c_0}{(r - \zeta)}, \quad r \rightarrow \zeta^+, \quad c_0 > 0, \quad (5.37)$$

a repulsive barrier absent in ordinary Schwarzschild or Reissner–Nordström backgrounds. Asymptotically ( $r \rightarrow \infty$ ), with  $R(r) \sim r$  and  $A(r) \rightarrow 1 - 8\pi G\eta^2$ ,

$$V_0(r) \sim (1 - 8\pi G\eta^2) \frac{\ell(\ell + 1)}{r^2} + O(r^{-3}). \quad (5.38)$$

Both limits are manifestly positive. The numerical solutions of Section III confirm that  $A(r) = B(r) > 0$  on the entire exterior domain (no horizon forms for the physically acceptable branch  $\tilde{\zeta} \geq 4\sqrt{3}$ ), so the angular-barrier term  $A(r)\ell(\ell + 1)/R^2(r)$  is strictly positive for  $\ell \geq 1$  throughout the exterior. The Born–Infeld correction  $V_{\text{BI}}(r)$  is non-negative because it arises from  $\bar{L}_{XX} > 0$ . The dilaton correction  $V_{\text{dil}}(r)$  may change sign, but its magnitude is suppressed relative to the angular barrier by a factor of order  $Q_m^2/(\beta_{\text{BI}} r^2)$ , which is small in the exterior. Hence  $V_0(r) > 0$  on the full domain  $r \in (\zeta, \infty)$ .

Note that for  $\ell = 0$  the spin-weighted harmonics  ${}_s Y_{0m}$  vanish identically for  $|s| \geq 1$ , so the helicity variables  $\psi_{\pm}$  vanish for  $\ell = 0$ : there are no propagating electromagnetic degrees of freedom in this sector, only the Gauss-law constraint fixing the total magnetic charge. The stability analysis is therefore vacuous for  $\ell = 0$ , and all statements about  $V_0 > 0$  apply for  $\ell \geq 1$ .

Because  $V_0(r) > 0$  everywhere in the exterior and the operator  $\mathcal{O} = -d^2/dr_*^2 + V_0$  is self-adjoint with respect to (5.33), its spectrum satisfies

$$\omega^2 = \frac{\langle \psi, \mathcal{O}\psi \rangle}{\langle \psi, \psi \rangle} = \frac{\int dr_* |\psi'|^2 + \int dr_* V_0 |\psi|^2}{\int dr_* |\psi|^2} > 0, \quad (5.39)$$

for any normalisable perturbation. There are no modes with  $\omega^2 < 0$ , and the purely magnetic self-gravitating Born–Infeld monopole is therefore **linearly mode stable**. The repulsive near-core barrier (5.37) provides an additional layer of stability, reflecting perturbations away from the core region by a potential wall that grows without bound as  $r \rightarrow \zeta^+$ .

## 2. Dyon: helicity mixing and the $2 \times 2$ Sturm–Liouville problem

For the dyonic background (4.8), both electric and magnetic fields are present and the pseudoscalar invariant  $\bar{Y} = \bar{F}_{\mu\nu} \tilde{F}^{\mu\nu}$  is non-vanishing:

$$\bar{Y} \propto \frac{Q_m Q_e^{\text{eff}}(r)}{R^4(r)} \neq 0. \quad (5.40)$$

The constitutive tensor  $\chi^{\mu\nu}{}_{\rho\sigma}$  therefore acquires an off-diagonal structure in the helicity basis: the term  $\partial^2 \mathcal{L} / \partial F_{\mu\nu} \partial F_{\rho\sigma}$  evaluated on the dyonic background couples  $\delta F$  components of opposite helicity through the background  $\tilde{F}$  tensor.

This is the mechanism identified in the GV framework [30]: when  $\bar{Y} \neq 0$ , the constitutive tensor mixes the two helicity sectors.

The off-diagonal coupling arises from the part of the constitutive tensor that is odd in the pseudoscalar invariant (5.40). After projection onto the helicity basis, the off-diagonal entry of the potential matrix takes the explicit form

$$\mathbb{W}(r) = -\frac{4 C_\ell(r)}{\beta \Delta^{3/2}(r)} \cdot \frac{e^{-2\Phi(r)} Q_m Q_e^{\text{eff}}(r)}{R^4(r)}, \quad (5.41)$$

where  $C_\ell(r) = \ell(\ell+1)/(2R^2(r))$  is the angular projection coefficient (exact from the spin-weighted harmonic identities), and  $\Delta(r)$  is the Born–Infeld discriminant evaluated on the background. The key structural feature is

$$\mathbb{W}(r) \propto Q_m [Q_e - (b(r) - b_0)Q_m], \quad (5.42)$$

so that in the purely magnetic limit ( $Q_e = 0$ ,  $b(r) = b_0$ ) one has  $Q_e^{\text{eff}} = 0$  and  $\mathbb{W}(r) = 0$ , recovering (5.34). More generally, the axion field  $b(r)$  partially screens the electric charge.

The full dyonic perturbation equation is the  $2 \times 2$  matrix system (5.30) with

$$\mathbf{V}(r) = V_0(r) \mathbf{1} + \mathbb{W}(r) \sigma_x, \quad (5.43)$$

where  $\sigma_x = \begin{pmatrix} 0 & 1 \\ 1 & 0 \end{pmatrix}$ . Since the static dyonic field profiles  $\Phi(r)$ ,  $b(r)$  and the metric functions are all real,  $V_0(r)$  and  $\mathbb{W}(r)$  are real functions and  $\mathbf{V}(r)$  is a real symmetric matrix. The operator  $\mathcal{O} = -d^2/dr_*^2 \mathbf{1} + \mathbf{V}(r)$  is self-adjoint and its eigenvalues  $\omega^2$  are real.

To establish positivity, diagonalise  $\sigma_x$  by  $U = \frac{1}{\sqrt{2}} \begin{pmatrix} 1 & 1 \\ 1 & -1 \end{pmatrix}$ :

$$U \mathbf{V} U^\dagger = \begin{pmatrix} V_0 + \mathbb{W} & 0 \\ 0 & V_0 - \mathbb{W} \end{pmatrix}. \quad (5.44)$$

Stability requires both eigenvalues  $V_0 \pm \mathbb{W}$  to be positive. The ratio  $|\mathbb{W}(r)|/V_0(r)$  satisfies

$$\frac{|\mathbb{W}(r)|}{V_0(r)} \leq \frac{2 e^{-2\Phi(r)} |Q_m Q_e^{\text{eff}}(r)|}{\beta \Delta^{3/2}(r) A(r) R^4(r)}. \quad (5.45)$$

Asymptotically ( $r \rightarrow \infty$ ): since  $Q_e^{\text{eff}}(r) \rightarrow Q_e - (b(\infty) - b_0)Q_m = 0$  by the boundary condition  $b_0 = -Q_e/Q_m$ , the ratio vanishes. Near the core ( $r \rightarrow \zeta^+$ ):  $\Delta(r) \rightarrow \infty$  because  $\bar{X} \sim R^{-4} \rightarrow \infty$ , so  $\Delta^{3/2}$  suppresses  $\mathbb{W}(r)$  faster than  $V_0(r)$  diverges—concretely,  $|\mathbb{W}| \sim (r - \zeta)^{+1/2}$  while  $V_0 \sim (r - \zeta)^{-1}$ , so  $|\mathbb{W}|/V_0 \rightarrow 0$  as  $r \rightarrow \zeta^+$ . Hence  $|\mathbb{W}(r)| < V_0(r)$  throughout the exterior, both eigenvalues  $V_0 \pm \mathbb{W}$  are positive definite, and  $\omega^2 > 0$  for all normalisable modes. The dyonic solutions are therefore **linearly mode stable**.

The helicity mixing does not introduce instabilities but rather produces a birefringent polarisation structure. In the monopole case the effective medium is isotropic and propagation is conformally equivalent to propagation in the background geometry. In the dyonic case,  $\bar{Y} \neq 0$  breaks this symmetry: the two helicities see different effective metrics,

$$g_{\text{eff}}^{\mu\nu}(\pm) \propto g^{\mu\nu} \pm \Delta g^{\mu\nu}(\bar{F}, \tilde{\bar{F}}), \quad (5.46)$$

an effect analogous to birefringence in anisotropic optical media. The off-diagonal term  $\mathbb{W}(r)$  quantifies this birefringence and vanishes precisely when  $Q_e^{\text{eff}} = 0$ , i.e. when the axion screens the electric charge completely.

## VI. DISCUSSION AND CONCLUSIONS

In this work, we have shown that global monopoles coupled to string-inspired dilaton, axion, and Born–Infeld (BI) sectors admit physically viable, self-gravitating magnetic monopole and dyon solutions. In particular, we constructed magnetically charged monopole configurations and their dyonic generalisations, demonstrating that the inclusion of dilaton and axion couplings converts the negative-mass behaviour of the standard global monopole into solutions with positive ADM mass. The resulting configurations are free of curvature singularities and event horizons, possess finite self-energy due to the non-linear BI electrodynamics, and satisfy the standard energy conditions. Furthermore, a linear perturbation analysis of the electromagnetic sector indicates that both the monopole and dyon solutions are

dynamically stable, with no evidence of unstable modes despite the presence of axion-induced helicity mixing in the dyonic case.

In particular, we constructed magnetically charged monopole configurations in which the dilaton field generates a secondary scalar hair, linking the magnetic charge to both the dilaton charge and the monopole mass. By employing an approximate analytic treatment according which the monopole possesses a de Sitter core, we imposed the Israel conditions to match the interior de Sitter spacetime to an exterior geometry, and identified the parameter regime in which the monopole mass becomes positive. Although this approximation is not uniformly accurate across the entire parameter space, our numerical analysis confirmed the existence of regular solutions and showed that the analytic approximate predictions capture the correct order of magnitude for both the mass and the magnetic charge.

A notable feature of the model is that the Born–Infeld sector renders the monopole self-energy finite, in contrast to the divergent behaviour encountered in Maxwell electrodynamics. This provides an additional indication that non-linear electrodynamics offers a natural framework for regulating classical field configurations with point-like sources. We further extended the analysis by incorporating a KR axion field, leading to dyonic generalizations of the monopole solutions. In this case, the axion coupling induces an effective electric charge through its interaction with the electromagnetic sector, resulting in a non-trivial dressing of the electric field. The resulting configurations are characterized by a combined charge  $Q^2 = Q_e^2 + Q_m^2$ , while the interior structure remains essentially unchanged under appropriate boundary conditions.

We also examined the mechanical stability and energy conditions of the solutions. Using the numerical configurations (in the monopole case), we showed that the energy density and pressures satisfy the null, weak, and strong energy conditions throughout spacetime. This behaviour is consistent with the absence of curvature singularities and horizons, and supports the physical viability of the solutions.

In addition, we performed a systematic linear mode stability analysis of the self-gravitating Born–Infeld monopole and dyonic solutions. We recall the key steps:

1. Starting from the perturbation of the vector potential  $\delta A_\mu$ , we constructed the gauge-invariant amplitudes  $(E_a, B)$  via the standard harmonic decomposition (5.21).
2. Projecting onto a null tetrad, we identified the two helicity modes  $\psi_\pm$  as the physically propagating degrees of freedom (5.25)–(5.26).
3. The linearised constitutive-tensor equation (5.28) reduces, after angular separation and introduction of the tortoise coordinate, to the Schrödinger-like master equation (5.30) with a real symmetric potential matrix.
4. Self-adjointness of the radial operator immediately implies a real spectrum  $\omega^2 \in \mathbb{R}$ .
5. Positivity of the effective potential  $V_0(r) > 0$  in the exterior, together with the rigorous bound  $|\mathbb{W}(r)| < V_0(r)$  derived from the explicit form  $C_\ell(r) = \ell(\ell+1)/(2R^2(r))$  and the BI saturation near the core, establishes  $\omega^2 > 0$  and hence linear stability for both monopoles and dyons.

For the magnetic monopole the analysis is particularly transparent: the two helicity sectors are completely decoupled, the effective potential is positive definite with a repulsive near-core barrier  $V_0 \sim (r - \zeta)^{-1}$  arising from the dilaton structure of the exterior geometry, and linear stability follows directly from the positivity argument (5.39).

For the dyon, the axion-induced  $F\tilde{F}$  coupling generates a non-trivial off-diagonal mixing term  $\mathbb{W}(r) \propto Q_m Q_e^{\text{eff}}(r)$ . The angular coefficient  $C_\ell(r) = \ell(\ell+1)/(2R^2(r))$  is computed from the spin-weighted harmonic projection, and the bound (5.45) shows rigorously that  $|\mathbb{W}(r)|/V_0(r) \rightarrow 0$  both asymptotically (because  $Q_e^{\text{eff}}(r) \rightarrow 0$  by the boundary condition  $b_0 = -Q_e/Q_m$ ) and near the core (because  $\Delta^{3/2} \rightarrow \infty$  suppresses  $\mathbb{W}$  faster than  $V_0$  diverges). Hence both eigenvalues  $V_0 \pm W$  are positive throughout, confirming stability without any additional assumption. The helicity mixing does not introduce instabilities but rather produces a birefringent polarisation structure in which the two circular polarisations propagate in slightly different effective geometries.

A notable structural result is the existence of a minimum nonzero magnetic charge in this model: as the de Sitter core radius approaches its lower bound  $\tilde{R}_{\text{ds}} \rightarrow \sqrt{6}$ , the monopole mass vanishes while the magnetic charge  $\tilde{Q}_m = \sqrt{\tilde{\zeta}\tilde{M}}$  remains finite, so the zero-mass configuration is held up entirely by magnetic charge and de Sitter core pressure. Overall, our results indicate that string-inspired dilaton, axion, and Born–Infeld couplings provide a natural framework in which global monopoles can be promoted to physically viable, self-gravitating magnetic monopoles and dyons with positive mass, finite energy, and stable dynamics.

Several directions for future work remain open. The gravitational sector perturbations (metric and dilaton fluctuations) have not been treated here; a full stability analysis would require coupling the electromagnetic GV system to the Regge–Wheeler–Zerilli equations for the metric and a coupled scalar equation for the dilaton. For the dyonic case, incorporating the gravitational back-reaction on the helicity-mixing structure could modify the effective potentials at

sub-leading order. Finally, it would be of interest to explore the phenomenological implications of these configurations, in particular their potential observational signatures in gravitational or electromagnetic contexts. Indeed, given the absence of compositeness in our MM, since our solutions are not characterised by constituent gauge bosons, in contrast to what happens in the electroweak [6–8] or low-mass Grand Unified MM [9], but they rather approximate Dirac-type structureless MM, one might hope of avoiding the strong suppression for the production of such MM at colliders, provided concrete relevant processes are identified. This will be looked at in future works. Moreover, such configurations may characterise phase transitions in the post-inflationary early Universe, and may have significant astrophysical or cosmological signatures, especially as a result of the interactions of the self-gravitating MM with gravitational waves or cosmic microwave background radiation.

*Affaire à suivre ...*

## ACKNOWLEDGMENTS

N.E.M. thanks the University of Valencia and its Theoretical Physics Department for a visiting Research Professorship supported by the programme Atracción de Talento INV25-01-15, during which this work has started. The work of N.E.M. and S.S. is supported in part by the Science and Technology Facilities Council (STFC) under the research grant no. ST/X000753/1, respectively. N.E.M. also acknowledges participation in the COST Association Actions CA21136 “Addressing observational tensions in cosmology with systematics and fundamental physics (CosmoVerse)” and CA23130 “Bridging high and low energies in search of Quantum Gravity (BridgeQG)”.

### Appendix A: Projection of the perturbation equations and derivation of the monopole radial potentials

This appendix gives a self-contained derivation of the radial Sturm–Liouville problem governing electromagnetic perturbations of the purely magnetic monopole background, making precise the origin of the structural contributions  $V_{\text{BI}}(r)$  and  $V_{\text{dil}}(r)$  that appear in the main text. Throughout we restrict to the purely magnetic case,

$$\bar{F}_{\theta\phi} = Q_m \sin\theta, \quad \bar{F}_{tr} = 0, \quad \bar{Y} := \bar{F}_{\mu\nu} \tilde{F}^{\mu\nu} = 0, \quad (\text{A1})$$

so that the two helicity sectors decouple from the outset.

#### 1. Linearised constitutive equation and Born–Infeld coefficients

The electromagnetic equations of motion  $\nabla_\mu P^{\mu\nu} = 0$ , with  $P^{\mu\nu} := -2\partial\mathcal{L}/\partial F_{\mu\nu}$ , are supplemented by the Bianchi identity  $\nabla_{[\mu} F_{\nu\rho]} = 0$ . Perturbing around the background,  $F_{\mu\nu} = \bar{F}_{\mu\nu} + \delta F_{\mu\nu}$ , the linearised relation is

$$\delta P^{\mu\nu} = \chi^{\mu\nu}{}_{\rho\sigma} \delta F^{\rho\sigma}, \quad \chi^{\mu\nu}{}_{\rho\sigma} = -2 \frac{\partial^2 \mathcal{L}}{\partial F_{\mu\nu} \partial F^{\rho\sigma}}, \quad (\text{A2})$$

and the linearised field equation is  $\nabla_\mu (\chi^{\mu\nu}{}_{\rho\sigma} \delta F^{\rho\sigma}) = 0$ .

The Born–Infeld Lagrangian depends on the two invariants  $X := F_{\mu\nu} F^{\mu\nu}$  and  $Y := F_{\mu\nu} \tilde{F}^{\mu\nu}$  through

$$\mathcal{L}_{\text{BI}} = 4\beta^2 e^{2\Phi} \left(1 - \sqrt{\Delta}\right), \quad \Delta := 1 + \frac{e^{-2\Phi}}{2\beta^2} X - \frac{e^{-4\Phi}}{16\beta^4} Y^2. \quad (\text{A3})$$

The relevant derivatives are

$$L_X := \frac{\partial \mathcal{L}}{\partial X} = -\frac{1}{\sqrt{\Delta}}, \quad L_{XX} = \frac{e^{-2\Phi}}{4\beta^2} \Delta^{-3/2}. \quad (\text{A4})$$

Since  $\bar{Y} = 0$  for the purely magnetic monopole, the background dependence enters only through

$$\bar{X}(r) = \frac{2Q_m^2}{R^4(r)}, \quad \bar{\Delta}(r) = 1 + \frac{e^{-2\Phi(r)}}{2\beta^2} \bar{X}(r), \quad (\text{A5})$$

giving

$$\bar{L}_X(r) = -\bar{\Delta}(r)^{-1/2}, \quad \bar{L}_{XX}(r) = \frac{e^{-2\Phi(r)}}{4\beta^2} \bar{\Delta}(r)^{-3/2}. \quad (\text{A6})$$

## 2. Gauge-invariant variables and helicity projection

We write the metric in 2 + 2 form,  $ds^2 = g_{ab}(x) dx^a dx^b + R^2(x) \gamma_{AB} d\theta^A d\theta^B$  with  $x^a = (t, r)$ , and decompose the vector-potential perturbation in scalar and vector spherical harmonics as in equations (5.19)–(5.20) of the main text. The gauge-invariant amplitudes are  $E_a := u_a - \partial_a u^{(e)}$  and  $B := u^{(o)}$ , and the mixed field-strength perturbation is

$$\delta F_{aA} = E_a \hat{D}_A Y_{\ell m} + (\nabla_a B) \hat{S}_A. \quad (\text{A7})$$

To extract the propagating helicity modes we introduce a complex null tetrad  $\{\ell^\mu, n^\mu, m^\mu, \bar{m}^\mu\}$  with  $\ell \cdot n = -1$ ,  $m \cdot \bar{m} = +1$ , all other inner products vanishing. The tetrad is adapted to the 2 + 2 split:  $\ell^\mu$  and  $n^\mu$  are purely radial,  $m^\mu = (0, m^A)$  and  $\bar{m}^\mu = (0, \bar{m}^A)$  are purely angular, with  $m^A$  and  $\bar{m}^A$  forming a complex null basis on  $S^2$  satisfying  $\gamma_{AB} m^A \bar{m}^B = 1$ . The area form acts on them as  $\hat{\epsilon}_A{}^B m_B = +i m_A$  and  $\hat{\epsilon}_A{}^B \bar{m}_B = -i \bar{m}_A$ , so they are eigenvectors of the Hodge dual on  $S^2$  with eigenvalues  $\pm i$ . The helicity variables are

$$\psi_+ := \ell^a m^A \delta F_{aA}, \quad \psi_- := \ell^a \bar{m}^A \delta F_{aA}. \quad (\text{A8})$$

Using (A7) together with the spin-weighted harmonic projections  $m^A \hat{D}_A Y_{\ell m} = -\sqrt{\ell(\ell+1)}/(\sqrt{2}R) {}_{+1}Y_{\ell m}$  and  $m^A \hat{S}_A = -i\sqrt{\ell(\ell+1)}/(\sqrt{2}R) {}_{+1}Y_{\ell m}$  (and their conjugates for  $\bar{m}^A$ ), one obtains

$$\psi_+ = -\frac{\sqrt{\ell(\ell+1)}}{\sqrt{2}R} \ell^a (E_a + i\nabla_a B) {}_{+1}Y_{\ell m}, \quad \psi_- = +\frac{\sqrt{\ell(\ell+1)}}{\sqrt{2}R} \ell^a (E_a - i\nabla_a B) {}_{-1}Y_{\ell m}. \quad (\text{A9})$$

Because  $\bar{Y} = 0$ , the constitutive tensor has no parity-odd dual-mixing term, so the off-diagonal helicity coupling vanishes ( $W(r) = 0$ ) and both helicities satisfy the same scalar equation. Dropping the helicity label,

$$-\frac{d^2\psi}{dr_*^2} + V_0(r)\psi = \omega^2\psi. \quad (\text{A10})$$

## 3. From weighted Sturm–Liouville to Schrödinger form

Before removing first-derivative terms, the projected radial equation takes the weighted Sturm–Liouville form

$$-\frac{d}{dr} \left( P(r) \frac{d\psi}{dr} \right) + Q(r)\psi = \omega^2 W(r)\psi, \quad (\text{A11})$$

where the kinetic coefficient is determined by the transverse constitutive response,  $P(r) \sim W(r) \sim -\bar{L}_X(r)$ , with geometric prefactors from the 2 + 2 decomposition. The potential  $Q(r)$  receives three contributions: (i) the angular barrier  $\propto \ell(\ell+1)$ ; (ii) terms from  $\bar{L}_X$  and  $\bar{L}_{XX}$  via the Born–Infeld constitutive tensor; (iii) terms from derivatives of  $A(r)$ ,  $B(r)$ ,  $R(r)$ ,  $\Phi(r)$  from the background geometry. This motivates the split  $Q(r) = Q_{\text{ang}} + Q_{\text{BI}} + Q_{\text{dil}}$ .

To reduce (A11) to Schrödinger form one introduces the tortoise coordinate

$$\frac{dr_*}{dr} = \sqrt{\frac{W(r)}{P(r)}} \quad (\text{A12})$$

and rescales  $\psi(r) = [P(r)W(r)]^{-1/4} u(r)$ , obtaining

$$-\frac{d^2u}{dr_*^2} + V_{\text{eff}}(r)u = \omega^2u. \quad (\text{A13})$$

In the case  $P(r) = W(r)$  this simplifies to

$$V_{\text{eff}}(r) = \frac{Q(r)}{P(r)} + \frac{1}{2} \frac{P''(r)}{P(r)} - \frac{1}{4} \left( \frac{P'(r)}{P(r)} \right)^2, \quad (\text{A14})$$

which makes the Born–Infeld contribution explicit: any radial variation of  $\bar{L}_X(r)$  generates additional terms through the derivatives of  $P(r)$ . After the Liouville transformation one writes

$$V_0(r) = A(r) \left[ \frac{\ell(\ell+1)}{R^2(r)} + \frac{V_{\text{BI}}(r) + V_{\text{dil}}(r)}{R^2(r)} \right], \quad (\text{A15})$$

where  $V_{\text{BI}}$  collects the terms whose coefficients originate from  $\bar{L}_X$ ,  $\bar{L}_{XX}$ , and  $\bar{X}(r) = 2Q_m^2/R^4(r)$ , while  $V_{\text{dil}}$  collects the terms generated by the dilaton-dependent metric functions  $R(r)$ ,  $\Phi(r)$ ,  $A(r)$ ,  $B(r)$  and their derivatives.

#### 4. Asymptotic behaviour of the effective potential

The analytic exterior background is

$$A(r) = B(r) = 1 - 8\pi G\eta^2 - \frac{2GM}{r}, \quad R(r) = \sqrt{r(r - \zeta)}, \quad \Phi(r) = -\ln\left(1 - \frac{\zeta}{r}\right), \quad (\text{A16})$$

giving  $\bar{X}(r) = 2Q_m^2/[r^2(r - \zeta)^2]$ . Near the inner boundary  $r \rightarrow \zeta^+$ , one has  $R^2(r) \sim \zeta(r - \zeta) \rightarrow 0$  while  $A(r)$  remains finite and positive, so the angular barrier dominates:

$$V_0(r) \sim \frac{A(\zeta) \ell(\ell + 1)}{\zeta(r - \zeta)} \equiv \frac{c_0}{r - \zeta}, \quad c_0 > 0, \quad (\text{A17})$$

a repulsive barrier that diverges at the dilaton singularity. Asymptotically,  $R(r) \sim r$  and  $A(r) \rightarrow 1 - 8\pi G\eta^2$ , so

$$V_0(r) = (1 - 8\pi G\eta^2) \frac{\ell(\ell + 1)}{r^2} + \mathcal{O}(r^{-3}). \quad (\text{A18})$$

Inside the de Sitter core,  $A_{\text{int}}(r) = B_{\text{int}}(r) = 1 - \Lambda_{\text{eff}} r^2/3$  with  $\Lambda_{\text{eff}} = 2\pi G\lambda\eta^4$ , and near  $r = 0$ ,

$$V_{\text{int}}(r) = \frac{\ell(\ell + 1)}{r^2} + \mathcal{O}(1), \quad r \rightarrow 0, \quad (\text{A19})$$

where the  $\mathcal{O}(1)$  term contains the positive de Sitter curvature correction  $m_{\text{eff}}^2 = 2\Lambda_{\text{eff}}/3$ . Both asymptotic limits of  $V_0$  are manifestly positive, and together with the positivity argument established in Section V C 1 they confirm linear stability without requiring explicit closed-form expressions for  $V_{\text{BI}}$  and  $V_{\text{dil}}$ .

### Appendix B: Mechanical Stability and Energy Conditions for the Purely Magnetic Born–Infeld Monopole

This appendix provides the static-mechanical checks that underpin the discussion in Section V A. We specialise throughout to the *purely magnetic* configuration  $Q_e = 0$ ,  $b = b_0$ , mirroring the logic developed for dyons but stripping away the electric sector so that the underlying structure of the stability argument is as transparent as possible.

#### 1. Stress–energy tensor in Born–Infeld electrodynamics

We begin by recording how the stress–energy tensor simplifies when only the magnetic field is present. With the purely radial monopole ansatz  $F_{\theta\varphi} = Q_m \sin\theta$  and  $F_{tr} = 0$ , the Born–Infeld constitutive factor takes the comparatively simple form

$$\Delta_{\text{mag}} = 1 + \frac{e^{-2\Phi} Q_m^2}{2\beta_{\text{BI}}^2 R^4},$$

and the stress tensor inherits azimuthal symmetry. Explicitly, the energy density and the two independent pressure components read

$$\rho_E^{(m)} = \frac{e^\Phi}{4\pi} \left[ \sqrt{\beta_{\text{BI}}^2 + \frac{e^{-2\Phi} Q_m^2}{R^4}} - \beta_{\text{BI}} \right], \quad p_R^{(m)} = \rho_E^{(m)} - \frac{e^{-\Phi} Q_m^2}{4\pi R^4 \sqrt{\beta_{\text{BI}}^2 + e^{-2\Phi} Q_m^2 / R^4}}, \quad p_\theta^{(m)} = p_\varphi^{(m)} = \rho_E^{(m)}. \quad (\text{B1})$$

The tangential pressures coincide with the energy density, a reflection of the magnetic Born–Infeld field’s residual isotropy in the angular directions, while the radial pressure is reduced by the characteristic Born–Infeld correction term.

#### 2. Energy conditions

With the explicit form (B1) in hand, it is straightforward to verify that the monopole field satisfies the standard energy conditions of general relativity throughout the exterior region  $R \geq R_{\text{core}}$ . One checks in turn that

$$\rho_E^{(m)} > 0, \quad \rho_E^{(m)} + p_R^{(m)} > 0, \quad \rho_E^{(m)} + p_R^{(m)} + 2p_\theta^{(m)} > 0,$$

so the null, weak, and strong energy conditions are all satisfied. The positivity of  $\rho_E^{(m)}$  follows immediately from the square-root structure of the Born–Infeld Lagrangian, which ensures that the energy density of a magnetic field always exceeds its Maxwell value; the remaining inequalities then follow by direct inspection of the pressure formulae.

### 3. Laue force–balance condition

Satisfying the energy conditions is necessary, but for the monopole to be mechanically self-consistent one must also check that the electromagnetic stress distribution admits an internal equilibrium. The appropriate criterion is the Laue condition, which demands that the integrated radial pressure exerted by each spherical shell vanishes:

$$\frac{d}{dR}(R^2 p_R^{(m)}) = 0. \quad (\text{B2})$$

Differentiating  $p_R^{(m)}$  as given in Eq. (B1) confirms that Eq. (B2) holds *identically*, not merely at a particular radius. This is a non-trivial consistency check: it reflects the fact that Born–Infeld electrodynamics, unlike Maxwell electrodynamics, furnishes a stress tensor that is already in mechanical equilibrium without any additional binding forces.

### 4. Shell stresses at the core boundary

The matching of the interior core geometry to the exterior monopole spacetime across the thin shell at  $R = \delta$  is governed by the Israel junction conditions. These yield the surface energy density  $\sigma_m$  and tangential pressure  $\Pi_m$ ,

$$\sigma_m = -\frac{\sqrt{1 - 2GM/\delta}}{2\pi\delta} + \frac{\sqrt{1 - \Lambda_{\text{core}}\delta^2/3}}{2\pi\delta}, \quad \Pi_m = \sigma_m/2.$$

The sign of these shell stresses is controlled by the dimensionless parameter  $\tilde{\zeta}$ , which encodes the competition between the gravitational compactness of the core and the repulsive effect of the interior cosmological constant. When  $\tilde{\zeta} > 4\sqrt{3}$ , the cosmological term dominates and both  $\sigma_m$  and  $\Pi_m$  are positive, so the shell itself satisfies the weak energy condition and the core–exterior junction is mechanically sound.

### 5. Summary

Taken together, the three checks above paint a consistent picture of the purely magnetic Born–Infeld monopole as a mechanically stable, self-gravitating object. The energy density and pressures derived from the Born–Infeld Lagrangian satisfy the null, weak, and strong energy conditions everywhere outside the core. The Laue force–balance condition (B2) is satisfied identically, confirming that no exotic binding forces are required to hold the field configuration together. Finally, for  $\tilde{\zeta} > 4\sqrt{3}$  the thin shell at the core boundary carries positive surface stresses, ensuring that the Israel matching is consistent with the weak energy condition and that the global solution is free of pathological shell matter.

- 
- [1] N. E. Mavromatos and V. A. Mitsou, Magnetic monopoles revisited: Models and searches at colliders and in the Cosmos, *Int. J. Mod. Phys. A* **35**, 2030012 (2020), arXiv:2005.05100 [hep-ph].
  - [2] G. 't Hooft, Magnetic Monopoles in Unified Gauge Theories, *Nucl. Phys. B* **79**, 276 (1974).
  - [3] A. M. Polyakov, Particle Spectrum in Quantum Field Theory, *JETP Lett.* **20**, 194 (1974).
  - [4] H. Georgi and S. L. Glashow, Unity of All Elementary Particle Forces, *Phys. Rev. Lett.* **32**, 438 (1974).
  - [5] A. K. Drukier and S. Nussinov, Monopole Pair Creation in Energetic Collisions: Is It Possible?, *Phys. Rev. Lett.* **49**, 102 (1982).
  - [6] Y. M. Cho and D. Maison, Monopoles in Weinberg-Salam model, *Phys. Lett. B* **391**, 360 (1997), arXiv:hep-th/9601028.
  - [7] Y. M. Cho, K. Kim, and J. H. Yoon, Finite Energy Electroweak Dyon, *Eur. Phys. J. C* **75**, 67 (2015), arXiv:1305.1699 [hep-ph].
  - [8] J. Ellis, N. E. Mavromatos, and T. You, The Price of an Electroweak Monopole, *Phys. Lett. B* **756**, 29 (2016), arXiv:1602.01745 [hep-ph].
  - [9] T. W. Kephart, G. K. Leontaris, and Q. Shafi, Magnetic Monopoles and Free Fractionally Charged States at Accelerators and in Cosmic Rays, *JHEP* **10**, 176, arXiv:1707.08067 [hep-ph].

- [10] T. W. B. Kibble, Topology of cosmic domains and strings, *Journal of Physics A: Mathematical and General* **9**, 1387 (1976).
- [11] I. K. Affleck and N. S. Manton, Monopole Pair Production in a Magnetic Field, *Nucl. Phys. B* **194**, 38 (1982).
- [12] O. Gould and A. Rajantie, Magnetic monopole mass bounds from heavy ion collisions and neutron stars, *Phys. Rev. Lett.* **119**, 241601 (2017), arXiv:1705.07052 [hep-ph].
- [13] O. Gould, D. L. J. Ho, and A. Rajantie, Towards Schwinger production of magnetic monopoles in heavy-ion collisions, *Phys. Rev. D* **100**, 015041 (2019), arXiv:1902.04388 [hep-th].
- [14] B. Acharya *et al.* (MoEDAL), Search for magnetic monopoles produced via the Schwinger mechanism, *Nature* **602**, 63 (2022), arXiv:2106.11933 [hep-ex].
- [15] P. A. M. Dirac, The Theory of magnetic poles, *Phys. Rev.* **74**, 817 (1948).
- [16] P. A. M. Dirac, Quantised singularities in the electromagnetic field,, *Proc. Roy. Soc. Lond. A* **133**, 60 (1931).
- [17] N. E. Mavromatos and S. Sarkar, On the stability of Born-Infeld-regularised electroweak monopoles, *Eur. Phys. J. Special Topics*, in press (2026), arXiv:2602.01921 [hep-th].
- [18] Y. M. Shnir, *Magnetic Monopoles*, Text and Monographs in Physics (Springer, Berlin/Heidelberg, 2005).
- [19] E. S. Fradkin and A. A. Tseytlin, Nonlinear electrodynamics from quantized strings, *Phys. Lett. B* **163**, 123 (1985).
- [20] N. E. Mavromatos and S. Sarkar, Finite-energy dressed string-inspired Dirac-like monopoles, *Universe* **5**, 8 (2018), arXiv:1812.00495 [hep-ph].
- [21] P. Svrcek and E. Witten, Axions In String Theory, *JHEP* **06**, 051, arXiv:hep-th/0605206.
- [22] N. E. Mavromatos and S. Sarkar, Magnetic monopoles from global monopoles in the presence of a Kalb-Ramond Field, *Phys. Rev. D* **95**, 104025 (2017), arXiv:1607.01315 [hep-th].
- [23] M. Barriola and A. Vilenkin, Gravitational Field of a Global Monopole, *Phys. Rev. Lett.* **63**, 341 (1989).
- [24] M. B. Green, J. H. Schwarz, and E. Witten, *Superstring Theory Vol. 1: 25th Anniversary Edition*, Cambridge Monographs on Mathematical Physics (Cambridge University Press, 2012).
- [25] M. B. Green, J. H. Schwarz, and E. Witten, *Superstring Theory Vol. 2: 25th Anniversary Edition*, Cambridge Monographs on Mathematical Physics (Cambridge University Press, 2012).
- [26] N. E. Mavromatos and S. Sarkar, Regularized Kalb-Ramond magnetic monopole with finite energy, *Phys. Rev. D* **97**, 125010 (2018), arXiv:1804.01702 [hep-th].
- [27] K. Farakos, G. Koutsoumbas, N. E. Mavromatos, and A. Zarafonitis, On internal mechanical properties of Electroweak Magnetic Monopoles and their effects on stability, *Eur. Phys. J. ST*, in press 10.1140/epjs/s11734-025-02083-z (2025), arXiv:2506.04872 [hep-th].
- [28] M. Laue, Zur Dynamik der Relativitätstheorie, *Annalen Phys.* **340**, 524 (1911).
- [29] N. E. Mavromatos and E. Winstanley, Aspects of hairy black holes in spontaneously broken Einstein Yang-Mills systems: Stability analysis and entropy considerations, *Phys. Rev. D* **53**, 3190 (1996), arXiv:hep-th/9510007.
- [30] R. Gervalle and M. S. Volkov, Electroweak monopoles and their stability, *Nucl. Phys. B* **984**, 115937 (2022), arXiv:2203.16590 [hep-th].
- [31] S. Arunasalam and A. Kobakhidze, Electroweak monopoles and the electroweak phase transition, *Eur. Phys. J. C* **77**, 444 (2017), arXiv:1702.04068 [hep-ph].
- [32] J. Ellis, N. E. Mavromatos, and T. You, Light-by-Light Scattering Constraint on Born-Infeld Theory, *Phys. Rev. Lett.* **118**, 261802 (2017), arXiv:1703.08450 [hep-ph].
- [33] J. Ellis, N. E. Mavromatos, P. Roloff, and T. You, Light-by-light scattering at future  $e^+e^-$  colliders, *Eur. Phys. J. C* **82**, 634 (2022), arXiv:2203.17111 [hep-ph].
- [34] V. A. Mitsou and E. Musumeci, Constraining magnetic monopoles and multiply charged particles with diphoton events at the LHC, (2026), arXiv:2604.07300 [hep-ph].
- [35] D. Harari and C. Lousto, Repulsive gravitational effects of global monopoles, *Phys. Rev. D* **42**, 2626 (1990).
- [36] W. Israel, Singular hypersurfaces and thin shells in general relativity, *Nuovo Cim. B* **44S10**, 1 (1966), [Erratum: *Nuovo Cim. B* 48, 463 (1967)].
- [37] N. Chatzifotis, N. E. Mavromatos, and D. P. Theodosopoulos, Global monopoles in the extended Gauss-Bonnet gravity, *Phys. Rev. D* **107**, 085014 (2023), arXiv:2212.09467 [gr-qc].
- [38] M. Born, Modified field equations with a finite radius of the electron, *Nature* **132**, 282.1 (1933).
- [39] M. Born, On the quantum theory of the electromagnetic field, *Proc. Roy. Soc. Lond. A* **143**, 410 (1934).
- [40] M. Born and L. Infeld, Foundations of the new field theory, *Proc. Roy. Soc. Lond. A* **144**, 425 (1934).
- [41] R. R. Metsaev, M. Rakhmanov, and A. A. Tseytlin, The Born-Infeld Action as the Effective Action in the Open Superstring Theory, *Phys. Lett. B* **193**, 207 (1987).
- [42] O. D. Andreev and A. A. Tseytlin, Partition Function Representation for the Open Superstring Effective Action: Cancellation of Mobius Infinities and Derivative Corrections to Born-Infeld Lagrangian, *Nucl. Phys. B* **311**, 205 (1988).
- [43] A. A. Tseytlin, *Born-Infeld action, supersymmetry and string theory*, edited by M. A. Shifman (1999) pp. 417–452, arXiv:hep-th/9908105.
- [44] R. G. Leigh, Dirac-Born-Infeld Action from Dirichlet Sigma Model, *Mod. Phys. Lett. A* **4**, 2767 (1989).
- [45] J. Dai, R. G. Leigh, and J. Polchinski, New Connections Between String Theories, *Mod. Phys. Lett. A* **4**, 2073 (1989).
- [46] J. Polchinski, Tasi lectures on D-branes, in *Theoretical Advanced Study Institute in Elementary Particle Physics (TASI 96): Fields, Strings, and Duality* (1996) pp. 293–356, arXiv:hep-th/9611050.
- [47] D. d'Enterria and G. G. da Silveira, Observing light-by-light scattering at the Large Hadron Collider, *Phys. Rev. Lett.* **111**, 080405 (2013), [Erratum: *Phys.Rev.Lett.* 116, 129901 (2016)], arXiv:1305.7142 [hep-ph].
- [48] M. Aaboud *et al.* (ATLAS), Evidence for light-by-light scattering in heavy-ion collisions with the ATLAS detector at the LHC, *Nature Phys.* **13**, 852 (2017), arXiv:1702.01625 [hep-ex].

- [49] A. M. Sirunyan *et al.* (CMS), Evidence for light-by-light scattering and searches for axion-like particles in ultraperipheral PbPb collisions at  $\sqrt{s_{NN}} = 5.02$  TeV, *Phys. Lett. B* **797**, 134826 (2019), arXiv:1810.04602 [hep-ex].
- [50] D. J. Gross and J. H. Sloan, The Quartic Effective Action for the Heterotic String, *Nucl. Phys. B* **291**, 41 (1987).
- [51] S. S. Yazadjiev, Einstein-Born-Infeld-dilaton black holes in non-asymptotically flat spacetimes, *Phys. Rev. D* **72**, 044006 (2005), arXiv:hep-th/0504152.
- [52] M. H. Dehghani and H. R. Rastegar Sedehi, Thermodynamics of rotating black branes in (n+1)-dimensional Einstein-Born-Infeld gravity, *Phys. Rev. D* **74**, 124018 (2006), arXiv:hep-th/0610239.
- [53] A. Sheykhi and N. Riazi, Thermodynamics of black holes in (n+1)-dimensional Einstein-Born-Infeld dilaton gravity, *Phys. Rev. D* **75**, 024021 (2007), arXiv:hep-th/0610085.
- [54] C. A. R. Herdeiro and E. Radu, Asymptotically flat black holes with scalar hair: a review, *Int. J. Mod. Phys. D* **24**, 1542014 (2015), arXiv:1504.08209 [gr-qc].
- [55] T. Karakasis, G. Koutsoumbas, A. Machattou, and E. Papantonopoulos, Magnetically charged Euler-Heisenberg black holes with scalar hair, *Phys. Rev. D* **106**, 104006 (2022), arXiv:2207.13146 [gr-qc].
- [56] D. P. Theodosopoulos, T. Karakasis, G. Koutsoumbas, and E. Papantonopoulos, Motion of particles around a magnetically charged Euler-Heisenberg black hole with scalar hair and the Event Horizon Telescope, *Eur. Phys. J. C* **84**, 592 (2024), arXiv:2311.02740 [gr-qc].
- [57] D. Garfinkle, G. T. Horowitz, and A. Strominger, Charged black holes in string theory, *Phys. Rev. D* **43**, 3140 (1991), [Erratum: *Phys.Rev.D* 45, 3888 (1992)].
- [58] S. Sur, S. Das, and S. SenGupta, Charged black holes in generalized dilaton-axion gravity, *JHEP* **10**, 064, arXiv:hep-th/0508150.